

**Epigenetic modulation of the UL97 gene product in
CMV-associated central nervous system tumors**

A Senior Honors Thesis

Presented in Partial Fulfillment of the Requirements for Graduation
with Distinction in Biological Sciences in the Undergraduate Colleges
of The Ohio State University

By

Stephanie D. Wright

The Ohio State University

June 2005

Project Advisor: Dr. Robert A. Baiocchi, Department of Internal
Medicine, Division of Hematology/Oncology, Comprehensive Cancer
Center

TABLE OF CONTENTS

| | <u>Page</u> |
|-------------------------------|-------------|
| 1. Abstract | 3 |
| 2. Introduction..... | 4 |
| 3. Materials and Methods..... | 11 |
| 4. Results..... | 18 |
| 5. Discussion..... | 24 |
| 6. Acknowledgments..... | 28 |
| 7. Literature Cited..... | 29 |

TABLE OF FIGURES

| <u>Figure</u> | <u>Page</u> |
|--|-------------|
| 1. HAT v. HDAC activity..... | 34 |
| 2. Dose-dependent HDACi induction of cell death at 48 hours..... | 35 |
| 3. Morphology of depsipeptide treatment in NB11 and NB11 CMV..... | 36 |
| 4. Morphology of HDACi 42 treatment in NB11 and NB11 CMV..... | 37 |
| 5. Depsipeptide induction of cell arrest and apoptosis in Gli3605..... | 38 |
| 6. HDAC1 and HDAC2 protein expression in human brain tumors..... | 39 |
| 7. Morphology of NB11 and NB11 CMV cells..... | 40 |
| 8. CMV alteration of fibroblast morphology..... | 41 |
| 9. PCR replication of the UL97 gene product..... | 42 |
| 10. Determination of vectors containing insert..... | 43 |
| 11. Mini prep for determination of correct insert size..... | 44 |
| 12. Sequencing of vector inserts..... | 45 |
| 13. Depsipeptide induction of UL97 and 18S in NB11-CMV..... | 46 |
| 14. HDACi 42 induction of UL97 and 18S in NB11-CMV..... | 47 |
| 15. PCNSL and consequences of EBV thymidine kinase expression..... | 48 |
| 16. Ganciclovir addition increases apoptosis..... | 49 |
| 17. Ganciclovir addition increases apoptosis (expt 2)..... | 50 |
| 18. Gli3605 tumor cells expressing luciferin in animal model..... | 51 |

ABSTRACT

Gliomas are the most common primary central nervous system (CNS) tumor and are associated with a particularly poor prognosis despite the advances of multimodality therapy. Recent work demonstrating an association between gliomas and cytomegalovirus (CMV) infection has led us to postulate that modulation of key viral gene products presents an attractive opportunity to selectively deliver therapy to this refractory CNS tumor. We hypothesize that drugs capable of targeting epigenetic processes will provide antitumor activity while simultaneously inducing viral gene products that can subsequently be targeted by a variety of agents including nucleoside analogues. Here we provide data demonstrating that drugs with histone deacetylase inhibitor (HDACi) activity facilitate glioblastoma cell cycle arrest and apoptosis *in vitro*. The glioma cell lines, Gli3605 and U251, and the neuroblastoma lines, NB11 and NB11 CMV were used in experiments to test our hypothesis. All lines treated with the HDACi depsipeptide or HDACi 42 underwent induction of programmed cell death in a dose-dependent fashion. However, the CMV-infected NB11 cell line demonstrated increased resistance to HDACi-mediated apoptosis. Treatment of the NB11 CMV cell line with doses of depsipeptide and HDACi 42, previously shown to inhibit histone deacetylase activity, resulted in the induction of the CMV protein kinase UL97 in a dose-dependent fashion. Addition of the nucleoside analogue ganciclovir (GCV) to HDACi-treated cells resulted in enhanced cell death that selectively occurred in NB11 CMV cells but not the parental line NB11 suggesting a CMV-specific effect. These data support consideration of combined use of histone deacetylase inhibitors and antiviral compounds in cytomegalovirus-associated malignant brain tumors. Studies are in progress to further characterize (i) mechanism(s) leading to enhanced HDACi-mediated UL97 expression, (ii) whether CMV-infected glioblastoma cell lines demonstrate similar findings and (iii) the effect of this combination treatment strategy in an *in vivo* model of PCNS-glioblastoma.

INTRODUCTION

Central nervous system tumors. In the United States alone, more than 200,000 people are diagnosed with primary or metastatic central nervous system tumors annually. Primary brain tumors encompass approximately 40,000 of these cases (1) and are the leading cause of solid tumor cancer death in children under the age of 20, the second leading cause in males ages 20-29, and the fifth leading cause in females ages 20-39 (2, 3). The projected five- and ten-year relative survival rates for malignant brain tumors are 28% and 24% respectively. However, there is a large variation in survival estimates among different types of brain tumors. Five-year survival rates exceed 85% for pilocytic astrocytomas but are less than 5% for glioblastomas (1, 4). Survival generally decreases with older age at diagnosis, and thus children and young adults have better survival for most histologies (1, 4). At present, the standard treatments for brain tumors include surgery, radiation therapy, and chemotherapy. These may be used either individually or in combination. The current dilemmas pertaining to these treatments are their toxicity, lack of effectiveness, and lack of precise targets which would allow for tumor-specific therapy.

Arising from the glial support cells in the CNS, gliomas comprise 77% of all malignant brain tumors (5). High grade malignant gliomas are aggressive CNS tumors that are divided into anaplastic astrocytomas (AAs, grade III) and glioblastoma (glioblastoma multiforme, GBM, grade IV) which can be distinguished based on their histopathologic features. Glioblastoma is the most

common type of glioma at 51.9% while astrocytomas represent 21.6% of all gliomas as a grade III cancer (1). The clinical manifestations of AA or GBM depend upon the position and size of the lesion within the CNS. High grade astrocytomas generate symptoms and signs by local brain invasion or compression and frequently present with increased intracranial pressure (ICP). Generalized symptoms such as headache and altered mental status are the result of increased ICP, which can be caused by mass effect obstructing cerebrospinal fluid outflow that frequently leads to hydrocephalus. Augmented ICP may lead to the classic clinical triad of headache, nausea, and papilledema. The most common focal signs and symptoms of high-grade gliomas are seizures and hemiparesis, while those less common include hemianopia, aphasia, apraxia, and neglect syndromes (6).

Once a malignant astrocytoma is suspected by a patient's symptoms and imaging, he/she often proceeds to surgical resection with an attempt at maximal preservation of neurological function. Unfortunately, the highly invasive nature of malignant gliomas often leads to poorly defined surgical margins and a high rate of local recurrence despite adjuvant chemoradiation (8, 9). Adjuvant focal involved RT has been shown to improve local control and survival after resection in at least two randomized trials and has become the standard of care (10, 11). Two meta-analyses showed that the benefit of procarbazine or carmustine to adjuvant RT is modest but significant compared to RT alone. Despite these advances, prognosis is still poor (12, 13). The average survival of patients with GBM is projected at 14 weeks with conservative therapy, 20 weeks with surgical

resection alone, 36 weeks with surgery plus radiation therapy, and 40 to 50 weeks with the addition of chemotherapy (7). It is therefore obvious that these treatments have only very limited effectiveness, and new approaches are needed.

Cytomegalovirus and cancer. Human cytomegalovirus (HCMV), a *B*-herpesvirus, is a major pathogen that is associated with a variety of diseases including encephalitis, neuroblastoma, glioblastoma (27), and colorectal cancer (14, 15). This virus is trophic for a wide range of cellular phenotypes and ubiquitously infects 50–90% of the adult human population. HCMV can be reinduced in individuals with chronic or acute inflammatory processes or immunosuppression. HCMV gene products can disrupt multiple cellular pathways involved in mutagenesis, angiogenesis, apoptosis, cell cycle, cell invasion, and host immune response (16-26). A large proportion (about 90%) of malignant gliomas are infected by HCMV, and multiple HCMV gene products are presented in these tumors (27).

Reactivation of an underlying persistent astrocytic or endothelial cell infection may lead to HCMV infection of glioma cells, or another possibility is *de novo* infection of glial cells that have accumulated cell cycle control defects. HCMV gene expression in a glial cell that does not lead to cell cycle arrest or apoptosis may perhaps promote clonal expansion without enacting a productive or cytopathic viral infection. Contemporary studies have indicated that long-term passage of HCMV in malignant glioma cells can result in variant strains with

minimal cytopathic effect. In latently infected glioma cells exposed to inflammatory stimuli or superinfected with other HCMV strains, HCMV can be reactivated (28, 29).

HCMV has been shown to replicate in many cell types, including fibroblasts, neuronal cells, epithelial cells, endothelial cells, and macrophages (30). Upon infection, the first genes to be transcribed by differential splicing of a primary transcript are the immediate early genes, which result in the two proteins IE1 p76 and IE2 p86 (31). These immediate early proteins autoregulate the major immediate early promoter (MIEP) and activate several downstream cellular promoters (32-41). The early genes of the virus are expressed as a result of immediate early expression, and these products are essential for DNA replication and lead to the expression of the late genes involved in virion assembly (44-46).

It has also been shown that IE1 and IE2 promote viral replication by inhibiting histone deacetylation at HDAC3, and IE 86 interacts with the p53 pathway by inhibiting Rb-mediated repression of transcription and consequently upregulating E2F (42-43). HCMV-associated cancer is linked to uncontrolled cell replication caused by loss of p53 activity (48).

Protein kinase UL97 and HDACi. pUL97 is a well-characterized target of antiviral therapy, as specific activity of pUL97 is required to convert ganciclovir into its monophosphorylated derivative (49, 50). Several reports have shown that UL97 acts as a ser/thr-specific protein kinase that can phosphorylate itself and other proteins (51, 52). It has recently been revealed that UL97 is critical for

efficient HCMV replication and has no natural nucleoside kinase activity (53, 54). These recent discoveries provide insight as to why UL97 is an excellent target for antiviral therapy (55). Interestingly, drugs with histone deacetylase inhibitor (HDACi) activity promote infection of normally non-permissive, undifferentiated cells, resulting in HCMV permissiveness by inducing the activity of the MIEP (47).

The acetylation status of core histones plays a pivotal role in regulating gene transcription through modulation of nucleosomal packaging of DNA (56-58). Nucleosomes are tightly compacted, which results in transcriptional silencing in the deacetylated form. Alternatively, with histone acetylation, the nucleosomal structure becomes relaxed, leading to transcription. There is a dynamic balance between these states with the activities of histone acetyltransferases (HATs) and histone deacetylases (HDACs) both of which are recruited to target genes (Figure 1). Improper regulation of this epigenetic system has been shown to cause inappropriate gene silencing, a key event in the pathogenesis of many forms of cancer (59-60). Because of this, it is highly likely that a class of drugs that inhibit histone deacetylase will promote CMV replication and, perhaps, derepress key promoters allowing for expression of viral proteins that can be targeted for tumor specific therapy.

Overview of depsipeptide and HDACi 42. Depsipeptide is a fermentation product from *Chromobacterium violaceum* first isolated by Fujisawa Company (61). Depsipeptide has demonstrated potent cytotoxic activity against human tumor cell lines and *in vivo* efficacy against both human tumor xenografts and

murine tumors, such as the subcutaneously implanted LOX melanoma, MX-1 mammary, NC1-H522 lung and UACC-62 melanoma (62). This compound shows an apparent lack of cross-resistance with vincristine, 5-FU, mitomycin-C and cyclophosphamide (62). The compound can decrease expression of c-myc oncogene by decreasing its mRNA expression in H-ras transfected NIH 3T3 cells but has no effect on H-ras mRNA expression (63). *In vitro* studies conducted by Fujisawa Pharmaceuticals Co. Ltd. demonstrate that depsipeptide has potent antiproliferative activity against 12 human cancer cells lines (IC50 values ranged between .55 and 4.44 nM but are less potent against cultured animal cells such as human HNF fibroblasts (IC50>10000 ng/ml)) (62). The *in vitro* potency of depsipeptide was confirmed in the NCI human tumor cell line drug screen (64).

The *in vivo* antitumor efficacy of depsipeptide was evaluated in several murine tumor and human tumor xenograft models by Fujisawa Pharmaceuticals Co, Ltd. (62) as well as by the NCI (64). The Southern Research Institute conducted studies in dogs which indicated that longer infusion times significantly diminish acute toxicity (64). Intravenous administration of 1.0 or 2.0 mg/kg *20 or 40 mg/m²) over 30 sec resulted in acute toxicity and death 2-8 days after drug administration in 5 of 14 dogs. When the same dose was administered over a four minute period, increases in LDH and CPK were seen but no deaths occurred. When the administration was prolonged to one hour infusion, the same doses led to minimal acute toxicity

HDACi 42 is a novel histone deacetylase inhibitor developed here at Ohio State University (Ching-Shih Chen Laboratory) which is 10,000-fold more potent than the parent molecule, phenylbutyrate. Preliminary *in vitro* and *in vivo* studies have shown that it has potent antitumor activity in a variety of cancers (61). Experiments are currently underway to determine its potency in a variety of *in vivo* cancer models.

We hypothesize that the use of histone deacetylase inhibitors will result in activation of replication and derepression of key promoter elements. This will allow for efficient expression of the UL97 protein in any CMV+ tumor cell, thus conferring sensitivity to the toxic effects of ganciclovir (GCV).

Thus far, the use of depsipeptide and HDACi 42 has been explored in glioblastoma lines. Additionally, UL97 has been induced with these compounds in the cell line NB 11 CMV, a neuroblastoma line used as a positively infected cytomegalovirus model. This induction has been shown to confer sensitivity to GCV and enhance HDACi-induced cell death. The preclinical development of this strategy is therefore justified, and steps are currently being taken to create a Gli3605 cell line constitutively expressing luciferase for use in a primary brain tumor model. Ultimately, we hope to move ahead into a clinical trial exploring the combinatorial use of HDACi and GCV.

MATERIALS AND METHODS

Cell lines. Gli3605 and U251 glioma tumor cells were obtained from the lab of Dr. E. Antonio Chiocca in the Department of Neurosurgery at Ohio State University. The NB11 and NB11 CMV neuroblastoma cell lines were obtained from Dr. James Waldman, Department of Pathology. All cells were cultured in RPMI-1640 containing 5-10% Fetal Bovine Serum, 1% Penicillin/Streptomycin. NB11 and NB11 CMV lines were specifically obtained for use as a 50% permissively infected model of CMV+ cancer (65).

Histone Deacetylase Inhibitors. Depsipeptide was obtained from John Wright (NCI, CTEP) with permission of Fujisawa Inc. The drug was used in concentrations of 0, 10, 50, 100, and 500 nM for experimental dose titrations and treatments of glioma and neuroblastoma cell lines. HDACi 42 was provided by Dr. Ching-Shih Chen, Department of Internal Medicine, The Ohio State University, and used in concentrations of 0, 0.5, 1, 2, 3, 5, and 10 μ M. Dimethyl sulfoxide (DMSO) was employed as the vehicle control at a dilution of 1:1000 from stock. 294 μ L was added per 3 mL. Following a four hour incubation in drug or vehicle control (DMSO), cells were washed and placed into standard growth medium (or experimental conditions).

Nucleoside analog. Ganciclovir (GCV), an antiviral compound, was diluted to a concentration of 100 μ g/mL from a 50 mg/mL stock. It was then utilized in combination with either Depsipeptide or HDACi 42 in an experiment including the NB11 and NB11 CMV+ lines. The purpose of this drug pairing was to explore the

combinatorial effects of histone deacetylase inhibitors and antivirals on CMV-infected cells.

Flow cytometry. Cells were analyzed for either cell cycle or apoptosis. Since all cells used were adherent, a separate 6 or 12-well plate was used for each time point. Media was pipetted from the plate and saved in collection tubes. Then, cells were washed with 1 mL phosphate buffered saline (PBS) per well, and the wash was also saved. To remove the cells, 300 μ L of Trypsin-EDTA was added, and the plates were incubated at 37°C for five minutes. Next, cells were removed by washing with 500 μ L PBS and placed in the labeled tubes with the aforementioned media and PBS collections. Samples were spun down in a centrifuge, and the supernatant was aspirated. Then, the cells were resuspended in 2 mL PBS to wash, spun again, and the PBS was aspirated. Each sample was resuspended in 300 μ L of 1X Annexin binding buffer for an apoptosis assay. Subsequently, 3 μ L of Annexin V (FL1) were added, and the samples were incubated on ice for 15 minutes. 5 μ L of Topro (FL 4) were added just prior to analysis by flow cytometry. In the case of cell cycle analysis, samples were resuspended in 400 μ L of PI (propidium iodide) buffer. All samples were analyzed using Becton-Dickinson's FACScalibur flow cytometer and CellQuest software.

RNA Isolation. Fibroblasts permissively infected with cytomegalovirus AD169 were obtained from Dr. James Waldman, Department of Pathology, The Ohio State University. At 72 hours post-infection, RNA was isolated from these cells

using TRIzol Reagent. According to the protocol provided by C6 Diagnostics™, the cells were lysed directly in the culture dish by adding 1 mL of TRIzol Reagent per 10 cm² of the dish, and the lysate was homogenized by passing it through a pipette several times. Then, the samples were incubated at room temperature (RT) for 5 minutes, and 0.2 mL chloroform was added for each mL of TRIzol originally added. Tubes were shaken vigorously for 15 seconds, incubated at RT for 2-3 minutes, and centrifuged at 12,000 x g for 15 minutes at 4°C. The resulting aqueous phase was transferred to a new tube and precipitated by the addition of 0.5 mL isopropyl alcohol per 1 mL TRIzol Reagent. Subsequently, the samples were incubated at RT for 10 minutes and centrifuged at 12,000 x g for 10 minutes at 4°C. The supernatant was withdrawn from the precipitate, and the resulting pellet was washed by adding 1 mL 75% ethanol for 1 mL TRIzol Reagent originally used. The sample was vortexed to mix, and centrifuged at 7400 x g for 5 minutes at 4°C. The RNA pellet was vacuumed and then air-dried for 20-30 minutes and resuspended by pipetting in 20 µL of RNase-free water and incubating at 55°C for 10 minutes. Following isolation, the concentration of the RNA was determined using a UV spectrophotometer, and the presence of 18S and 28S ribosomal RNA species was evaluated by agarose gel electrophoresis. All samples were stored at -80°C.

Reverse Transcription and PCR. A reverse transcription was performed using a kit purchased from Invitrogen™, which included the MMLV-RT enzyme. RT-PCR was performed following manufacturer's suggestions. Briefly, 1.5 µL

random primers, 2 uL RNA (1.165 ug/uL), and 11.5 uL H₂O were combined, placed on a PCR block at 70°C for 2 minutes, and then immediately placed on ice. Subsequently a master mix containing 6.0 uL 5X Buffer, 3.0uL DTT (0.1 M), 1.5 uL dNTP mixture (10 mM each), 1.5 uL MMLV-RT, and 1.0 uL H₂O was added for a total volume of 30 uL. The samples were placed on a PCR block for one cycle of 60 minutes at 42°C, 5 minutes at 94°C, and 4°C indefinitely. The resulting cDNA was stored at -20°C.

The Polymerase Chain Reaction (PCR) was performed using the TaKaRa LA Taq™ kit from Takara Bio Inc. (Japan). The primers used were 5' (UP) EcoRI-CCGGAATTCCCATGTCCTCCGCACTTCGGTCTCG-3' and 5' (DN) Xho-GGCCTCGAGTTACTCGGGGAACAGTTGGCGGCA-3'. To achieve a final volume of 25 uL, 0.25 uL TaKaRa LA Taq™ enzyme, 12.5 uL 2X GC Buffer I, 4 uL dNTP mixture (2.5 mM each), 5.25 uL H₂O, 1 uL each of forward and reverse primers, and 1uL cDNA were combined in a PCR tube. The samples were placed on a PCR block for 30 cycles of 94°C/1 min., 94°C/30 sec., 60°C/30 sec., 72°C/2 min., and 72°C/5 min. with a 4°C indefinite hold.

Chemical transformation and sequencing. The PCR products were mixed with Blue Juice^R and run on a 1% agarose gel with 2.5 uL Ethidium Bromide to determine the correct size of 2.1kB. The products were then cut out of the gel and purified using Qiagen's™ Gel Purification Protocol. Next, the ligation was performed using the TOPO TA Cloning^R Kit provided by Invitrogen™. Combined in a tube were 4 uL PCR product, 1uL salt solution, and 1uL TOPO^R vector,

which were incubated 5 minutes at RT. One 50 uL vial of One Shot^R Top 10 competent *E. Coli* cells was thawed on ice for each ligation product, and 4 uL of this product was added to each vial of cells. The vials were then incubated on ice for 30 minutes followed by a 30 second incubation at 42°C in a water bath. Subsequently, the vials were returned to ice, and 250 uL S.O.C. medium was added to each, after which they were shaken for one hour at 225 rpm and 37°C. LB agar plates containing 50ug/mL ampicillin were spread with 20-200 uL of reaction mixture and inverted at 37°C overnight. Colonies were picked, all of which grew out in liquid TB medium with ampicillin.

To determine correct vector-containing-insert size, 30 uL mini dye was added to each eppendorf^R tube along with 30 uL phenochloroform and 50 uL transformed cells. The tubes were then vortexed and spun at max speed for 2-3 minutes. The 1% agarose gel with 2.5uL EtBr was loaded with 50 uL of sample from the resulting aqueous layer. Supercoil DNA marker was used as a marker. All samples were again selected, and mini preps were performed on the 800 uL of each colony according the Eppendorf Fast Plasmid MiniTM protocol. The resulting DNA vector samples were then digested using 2 uL EcoRI, 2uL Buffer 3, 11uL H₂O, and 5 uL DNA at 37°C for one hour. The products were run on a gel to check for correct fragment and vector size, 2.1 kB and 3.9 kB, respectively. Clones with inserts of the correct size were sent for sequencing using M13 forward and reverse primers with T3 and T7 polymerases, and all clones returned 97-98% homology to the UL97 CMV protein kinase, as determined using NCBI Nucleotide Blast software.

Immunohistochemical analysis. In preparation for staining, three cytopins of both NB11 and NB 11 CMV+ were made. Each slide held approximately 2000 cells. All six were fixed in ice-cold acetone. According to the protocol supplied by Dr. James Waldman, cells were rehydrated in TBS (OSU Stores) and then placed in 1:5 horse serum (Gibco™) diluted with TBS to block non-specific binding. Subsequently, the serum was drained from the slides, and they were placed in a humidity chamber. The primary antibodies, anti-CMV IE and anti CMV-gB, were diluted 1:200 and 1:300, respectively, in 2% Horse serum in TBS (Antibody Dilution Solution, ADS). These were added to all slides in the humidity chamber and incubated at 37°C for 30 minutes. The excess antibody was then removed, and the slides were rinsed in TBS. Subsequently, the secondary antibody, Biotinylated Horse Anti-Mouse IgG (BHAM) (Vector Laboratories, Burlingame, CA) was placed on the slides at a dilution of 1:200 in ADS. Slides were incubated at 37°C for 10 minutes and rinsed with TBS three times. Next, Horseradish Peroxidase Avidin D (HP) (Vector Laboratories) was applied to the slides at a dilution of 1:500 in ADS, and slides were incubated at 37°C for 10 minutes. Meanwhile, AEC substrate solution was prepared by addition of one tablet AEC to 2.5 mL N,N-Dimethylformamide and dilution in 47.5 mL acetate buffer and 25 uL H₂O₂ (30%). Following incubation, slides were rinsed three times in TBS and incubated in acetate buffer 5 minutes. All slides were developed in AEC substrate solution, and the reaction was stopped with acetate buffer. Slides were then coverslipped with glycerin jelly (AFIP formula, OSU Stores) and examined microscopically.

Generation of glioblastoma cell lines constitutively expressing luciferase.

To generate a GBM cell line that could be used in an *in vivo* model of human PCNS tumor, the Gli3605 cell line was transfected with the pGL3-Luc (or control pGL3) plasmid vector. pGL3 is a circular plasmid that constitutively drives expression of firefly luciferase and the neomycin resistance gene. To determine a toxic dose of neomycin, Gli3605 cells were plated in the presence of increasing concentrations of G418 (neomycin from Gibco™ Inc). After one week, we found that 95% of Gli3605 cells had died (by trypan blue dye exclusion) when plated in presence of 1.5 mg/ml G418. When assessed at 2 weeks, 100% of Gli3605 cells had died (compared to 90% of cells plated at 1.25 mg/ml). Therefore, we chose this concentration as the condition to select positive transfectants. We utilized the Lipofectamine 2000 reagent (Invitrogen™ Inc.) to transfect pGL3-Luc and control vector into Gli3605 cells following manufacturer's recommendations. Cells were expanded for 48 hours after transfection to allow for adequate neo resistance gene expression and then placed into selection media containing 1.5 mg/ml of G418. After expanding in selection media for 3 weeks, pGL3-Luc and pGL3 polyclonal populations demonstrated 100% viability (compared to 0% viability of control Gli3605). We then subcloned G418 resistant cells (1 cell / well) into 96 well plates and allowed clones to expand. 30 single clones were isolated and checked for luciferase expression. The five brightest clones were then expanded and tested in the presence of luciferin for fluorescence *intensity in vitro* and *in vivo* utilizing the IVIS system.

RESULTS

Depsipeptide and HDACi 42 can induce apoptosis in human glioblastoma and neuroblastoma cell lines. To investigate the effects of the two histone deacetylase inhibitors on each of the four cell lines, a dose titration was performed. For each cell line, 250,000 cells were plated per condition. Depsipeptide (DP) was added at concentrations of 0, 10, 50, 100, and 500 nM and washed out after 4 hours; HDACi 42 was used at concentrations of 0, 1, 2, 3, and 5 μ M and either washed out after 4 hours or left in for duration of the experiment. DMSO was used as the vehicle control. At 24 and 48 hours, cells were harvested and stained with either propidium iodide or annexin V/topro III and analyzed by flow cytometry. In the glioma lines, U251 and Gli3605, and the neuroblastoma lines, NB11 and NB 11 CMV, treatment with DP and HDACi 42 resulted in dose-dependent induction of apoptosis (Figure 2). In DP 500nM, apoptosis percentages were as follows: NB11 CMV-27.7%, NB11-14.5%, Gli3605-76.9%, and U251-43.3%. When 5 μ M HDACi 42 was used, percentages were: NB11 CMV-51.8%, NB11-68.5%, Gli3605-21.5%, and U251-40.5%. Changes in cellular morphology consistent with programmed cell death were also documented in NB11 and NB11 CMV lines (Figures 3 and 4). For both DP and HDACi 42, large, detached floating foci of cells were seen, and the amount of foci visibly increased with drug dose concentration.

Depsipeptide induces cell cycle arrest in Gli3605 at 24 hours. In addition to the apoptotic capabilities of DP, another dose titration showed that the drug induced cell cycle arrest in GBM cell lines. Concentrations of 0, 10, 50, 100, and 500 nM DP were tested, and a cell cycle analysis was performed at 24 and 48 hours using PI (propidium iodide) buffer, Becton-Dickinson's FACScalibur flow cytometer, and CellQuest software. The results demonstrate 47-58% of cells arrested in G2/M at 24 hours, followed by an exit from arrest and an average of 49% apoptosis at 48 hours (Figure 5).

Histone deacetylase 1 and 2 protein expression is increased in human brain tumors. We consistently observed notable variation amongst different cell lines in susceptibility to HDACi-induced apoptosis. One potential mechanism contributing towards resistance to the proapoptotic effects of HDACi may involve upregulation of HDAC enzymes. Western blot and Ponceau staining procedures targeting HDAC1 and 2 were performed on twelve patient brain tumor samples by the lab of Dr. Antonio Chiocca in the Department of Neurological Surgery at OSU College of Medicine and Public Health. These results show the elevated expression of HDAC1 and HDAC2 proteins in some GBM tumors (Figure 6). In data not shown, the levels of HDAC1 and 2 proteins directly correlated with HDAC activity (personal communication E.A. Chiocca).

CMV alters cellular morphology. NB11 and NB11 CMV were useful as CMV positive and negative cancer lines to evaluate the consequences of HDACi in CMV + cancer (Figure 7). The morphology of NB11 cells shows spindle-like cells with dendritic-like projections, and they tend to aggregate into foci. The NB11 CMV cells, however, are larger, with fewer projections, absence of cellular aggregation and grow as a monolayer. NB11 CMV cells appear to form syncytia, and inclusion bodies are also evident, which are likely secondary to CMV pathogenic effect on the line. Both of these cell lines were stained with IE and gB antibodies using immunohistochemical staining techniques (data not shown). The staining confirmed that the CMV negative nature of NB11 cells while the NB11 CMV cells were 50% positive for infection. The third cell line employed for use with CMV was the fibroblast line MRC5 (Figure 8). This cell line was infected with CMV (strain AD169) for the purpose of isolating RNA to clone the UL97 gene product. It is apparent that the uninfected fibroblasts have a long, flat, spindle-like shape, while the infected cells draw in their extensions and develop a more rounded appearance.

Cloning of UL97. Following RNA isolation from the MRC5 fibroblasts, a reverse transcription was performed to obtain cDNA. The primers specific for UL97, 5' (UP) EcoRI-CCGGAATTCCATGTCCTCCGCACTTC GGTCTCG-3' and 5' (DN) Xho-GGCCTCGAGTTACTCGGGGAACAGT TGGCGGCA-3', were then utilized in PCR (Figure 9). The resulting 2.1 kB products were purified and ligated into the TOPO^R vector, which was checked for correct size with insert by lysing with

phenochloroform and running on a 1% agarose gel with Supercoil DNA marker (Figure 10). Finally, a mini prep was performed using the Eppendorf Fast Plasmid Mini™ protocol (Figure 11). This verified the proper insert and vector sizes of 2.1 kB and 3.9 kB, respectively. Four clones of the correct sizes were selected for sequencing, and all were verified to be 97-98% homologous to the UL97 protein kinase (Figure 12). Once isolated, the UL97 gene was cloned into the bacterial expression vector pGEX (Not1 and EcoR1 sites) for expression and isolation of large amounts of UL97 to evaluate phosphorylation assays using novel nucleoside analogues synthesized in collaboration with Dr. Werner Tjarks from the OSU College of Pharmacy (not shown).

The UL97 gene product is induced by HDACi. We have previously demonstrated that expression of viral kinase proteins in CNS tumors from patients with Epstein-Barr virus positive tumors presents an attractive opportunity to deliver selective, anti-tumor activity (66 and figure 15). Basal levels of the protein kinase UL97 transcript were found to be difficult to amplify with one round of PCR suggesting that this gene product is not commonly expressed in CMV+ tumor lines. Our lab has previously demonstrated that several EBV gene products are induced following treatment with hypomethylating agents and HDACi supporting the notion that herpesvirus gene expression is tightly regulated and subject to transcriptional silencing. We therefore utilized HDACi in an attempt to induce the expression of the UL97 protein with the intent to confer sensitivity to the antiviral drug ganciclovir. NB11 and NB11 CMV cells were

plated in the presence of media containing DP and HDACi 42. DP was used in concentrations of 0, 10, 50, and 100 nM and washed out after a 4 hour incubation; HDACi 42 was used in concentrations of 0,1, 5, and 10 uM and remained in the media. At 48 hours, the cells were harvested, and RNA was isolated for each condition. A reverse transcription was performed on all samples, and the resulting cDNA was amplified by PCR to determine the levels of UL97 and 18S transcript present for each condition (Figures 13 and 14). PCR was performed on 2.5 uL cDNA and cDNA diluted 1:10 (for semiquantitative analysis), and the products were loaded on a 1% agarose gel for evaluation of relative amounts of amplified products. For NB11 CMV, the levels of UL97 increased relative to the 18S band intensity as doses of each drug increased. For NB11, there was no detectable UL97 amplified. Real time quantitative PCR studies are presently underway to verify our findings.

Depsipeptide enhances NB11 CMV sensitivity to Ganciclovir *in vitro*. To determine if enhanced expression of the UL97 gene product was associated with enhanced sensitivity to the antiviral drug GCV, we performed a series of experiments evaluating combination HDACi / GCV therapy in NB11 and NB11 CMV cells. Cell lines were plated in 0, 50, and 100nM DP, which was washed out after a 4 hour incubation. Half of the samples were then treated with 100ug/mL GCV and allowed to incubate for 24, 48 and 72 hours. At 24, 48 and 72 hours, cells were harvested, stained with Annexin V/Topro III and analyzed for apoptosis on Becton-Dickinson's FACscalibur flow cytometer using CellQuest

software. The results showed enhanced sensitivity to GCV for NB 11 CMV (Figure 16 and 17). While the sensitivity of NB11 was also enhanced, the same level of synergy was not achieved. Depsipeptide acts by increasing transcription of the UL97 protein kinase, which may then phosphorylate the antiviral GCV resulting in the induction of apoptosis.

DISCUSSION

While modern advances in surgery, radiotherapy and targeted therapy have led to enhanced survival in multiple solid and hematologic malignancies, conventional and experimental therapies for primary CNS tumors have not improved. Thus, it is necessary to explore novel therapeutic approaches that address new targets and newly discovered regulatory mechanisms that contribute to cellular transformation. The field of epigenetics has identified several mechanisms that contribute to tumor suppressor gene silencing. Thus, drugs that interfere with epigenetic processes have become attractive candidates to test in preclinical and clinical trials. In addition, HDACi and hypomethylating agents have recently been shown to contribute to covalent modification of histone proteins and DNA in several large herpesvirus genomes such as EBV and CMV. Drugs that target these epigenetic processes have been shown to promote gene expression of viral gene products that are normally tightly regulated or silenced. The association tying CMV infection with the most common primary CNS tumor, GBM, therefore presents an attractive opportunity to utilize the virus as a tool to aid in enhancing tumor-specific therapy.

Gliomas are accountable for 77% of all malignant brain tumors, 51.9% of which are glioblastomas (5). Currently, the standard treatments for brain tumors include surgery, radiation therapy, and chemotherapy, which may be used either individually or in combination. These treatments present problems because of their toxicity, lack of effectiveness, and lack of precise targets which would allow

for tumor-specific therapy. Because the average survival rates of patients with GBM is projected at only a little over a year, and five-year survival rates are less than 5%, the results of this paper could indicate the beginning of a novel tumor therapy strategy (1, 4, 7).

A majority (about 90%) of malignant gliomas are infected by HCMV, and multiple HCMV gene products are presented in these tumors (27). This gives justification to the strategy of using HDACi, which act to derepress viral gene promoters that are normally silenced secondary to tight histone-induced chromatin condensation. The amino tails of histone proteins are deacetylated by corepressor proteins like HDAC1 and 2 leading to “tight” chromatin structure. Drugs that inhibit HDAC activity allow for HAT protein activity to predominate resulting in acetylation of histones and “loose” chromatin structure. This promotes multimeric protein complexes (SWI/SNF) that remodel chromatin to access promoter regions, allowing for transcription factor association and gene expression. Currently, depsipeptide has been shown in various studies to have cytotoxic, antiproliferative activity against at least 12 human cancer cell lines both *in vivo* and *in vitro* (62, 64). Preliminary *in vitro* and *in vivo* studies have also shown that HDACi 42 has potent antitumor activity in a variety of cancers (61). Drugs with HDACi activity are attractive candidates for CMV+ GBM given the associated antitumor activity and the ability to enhance expression of viral gene products that can be targeted. Because the CMV protein kinase UL97 appears to be “silenced” in most models and is capable of phosphorylating GCV, we

hypothesized that HDACi would contribute to UL97 transcriptional activation, thereby providing a viral protein to target with nucleoside analogues.

Cytomegalovirus-infected brain tumor cells that are exposed to depsipeptide or HDAC-42 are sensitized to the antiviral ganciclovir, which adds to the antitumor effect of HDACi. We show here that HDACi leads to enhanced UL97 transcription that is associated with this enhanced antitumor effect. Cytomegalovirus is responsible for changes in morphology and, perhaps, plays a role in oncogenesis through cellular transformation and immortalization (16-26). It also clear that HDACi alone facilitate apoptosis and cell cycle arrest in both glioma and neuroblastoma lines. Our preliminary studies show that the greatest amount of apoptotic activity appears to be at 48 hours after treatment, and G2/M cell cycle arrest appears at 24 hours. While this project is early in its development, our findings may have implications that apply to both oncology and infectious disease problems. CMV is a ubiquitous infectious agent associated with a wide variety of pathology. It will be interesting to test whether HDACi alone or in combination with other epigenetic agents (5-Aza, Decitabine) lead to more impressive expression of the UL97 gene product conferring greater sensitivity to GCV.

We are presently working towards clarifying the mechanism by which HDACi leads to UL97 expression. We are also utilizing SiRNA and antisense RNA experiments to “knock out” UL97 expression to see if this protein is vital to the enhanced antitumor effect of HDACi + GCV. In addition, we are collaborating with Dr. Werner Tjarks (OSU Pharmacy) to test novel nucleoside analogues with

recombinant UL97 synthesized in our lab. We are extending the findings from our neuroblastoma CMV+ model to a CMV+ GBM model. We are about to begin generating CMV+ Gli3605 and U251 glioma lines to perform experiments examining the effects of HDACi on cell death, UL97 gene activation, and combination HDACi and GCV therapy treatment. The epigenetic regulation of UL97 and prosurvival mechanisms that are activated following HDACi treatment will also be examined. Finally, we have developed an *in vivo* model of GBM using Gli3605 cells that have been engineered to constitutively express luciferase (Figure 18). This preclinical model will allow us to use the *in vivo* imaging system to monitor CNS tumor burden in real time during our therapeutic trials. If this trial proves successful, a phase one trial in patients with CMV+ GBM will be pursued.

ACKNOWLEDGEMENTS

First, I would like to thank Dr. Robert Baiocchi and Dr. Navin Wadehra for all of their help, patience and willingness to teach and guide me through my experiments and thesis. I would also like to express gratitude to them for creating an enjoyable research environment that facilitated valuable learning. Additionally, I would like to thank Dr. James Waldman, Dr. Marshall Williams, Dr. Michael Caligiuri, Dr. Antonio E. Chiocca, Dr. Ching-Shih Chen, Dr. Tom Liu, Tim Ryan, Baiocchi lab, and my family for all of their extra help, support, and instruction. This has been an unforgettable experience, and I will carry it with me always.

LITERATURE CITED

1. Report, *Primary Brain Tumors in the United States, 1992-1997*.
2. [SEER](#) *Pediatric Monograph*, 1975-94, Table XXVII-7.
3. Jemal, A., Murray, T., Samuels, A. Cancer Statistics, 2003. January/February 2003. Vol. 53, No. 1. CA: A Cancer Journal for Clinicians. American Cancer Society. Page 5-26.
4. Ries, L.A.G., Eisner, M.P., Kosary, C.L., Hankey, B.F., Miller, B.A., Clegg, L., Edwards, B.K. (eds.) *Seer Cancer Statistics Review, 1973-1999*: National Cancer Institute, Bethesda, MD, 2002.
5. CBTRUS Report, 1997-2001.
6. Batchelor, T. *Clinical manifestations and diagnosis of high grade malignant astrocytoma*. UpToDate. Ver. 13.1, 2005.
7. Laws, E.R., Parney, I.F., Huang, W, et al. *Survival following surgery and prognostic factors for recently diagnosed malignant glioma: data from the Glioma Outcomes Project*. J Neurosurg 2003; 99:467.
8. Giese, A., Bjerkvig, R., et al. *Cost of migration: invasion of malignant gliomas and implications for treatment*. J Clinical Oncology 2003 April 15; 21(8): 1624-36.
9. Albert, F.K., Forsting, M., et al. *Early postoperative MRI after resection of malignant glioma: objective evaluation of residual tumor and its influence on regrowth and prognosis*. Neurosurgery 1994 Jan; 34(1): 45-60.
10. Walker, M.D., Green, S.B., et al. *Randomized comparisons of radiotherapy and nitrosoureas for the treatment of malignant glioma after surgery*. New England Journal of Medicine 1980 Dec 4; 303 (23): 1323-9.
11. Anderson, A.P. *Postoperative irradiation of glioblastomas. Results in a randomized series*. Acta Radiol Oncology Radiat Phys Biol. 1978; 17(6): 475-84.
12. Fine, H.A., Dear, K.B., et al. *Meta-analysis of radiation therapy with and without adjuvant chemotherapy for malignant gliomas in adults*. Cancer 1993 Apr 15; 71(8): 2585-97.
13. Stewart, L.A., *Chemotherapy in adult high-grade glioma: a systemic review and meta-analysis of individual patient data from 12 randomized trials*. Lancet 2002 Mar 23; 359 (9311): 1011-8.
14. Howley, P.M., Ganem, D., and Kieff, e. *DNA viruses*. In: V.T. De Vita, Jr., S. Hellman, and S.A. Rosenberg (eds.), *Cancer: Principles and Practice of Oncology*: 168-173. Philadelphia: Lippincott Williams and Wilkins, 2001.
15. Britt, W.J. and Alford, C.A. *Cytomegalovirus*. In: B.N. Fields, D.M. Knipe, and P.M. Howley (eds.), *Fields Virology*, Ed. 3: 2493-2523. New York: Raven Press, 1996.
16. Fritschy, J.M., Brandner, S., et al. *Brain cell type specificity and gliosis-induced activation of the human cytomegalovirus immediate-early promoter in transgenic mice*. J. Neurosci., 16: 2275-2282, 1996.

17. Wolff, D., Sinzger, C., Drescher, P., Jahn, G., and Plachter, B. *Reduced levels of IE2 gene expression and shutdown of early and late viral genes during latent infection of the glioblastoma cell line U138-MG with selectable recombinants of human cytomegalovirus.* Virology, 204: 101-113, 1994.
18. Doniger, J., Muralidhar, S., and Rosenthal, L.J. *Human cytomegalovirus and human herpesvirus 6 genes that transform and transactivate.* Clin. Microbiol. Rev., 12: 367-382, 1999.
19. Shen, Y., Zhu, H., and Shenk, T. *Human cytomegalovirus IE1 and IE2 proteins are mutagenic and mediate "hit-and-run" oncogenic transformation in cooperation with the adenovirus E1A proteins.* Proc. Natl. Acad. Sci. USA, 94: 3341-3345, 1997.
20. Zhu, H., Shen, Y., and Shenk, T. *Human cytomegalovirus IE1 and IE2 proteins block apoptosis.* J. Virol. 69: 7960-7970, 1995.
21. Loenen, W.A., Bruggeman, C.A., and Wiertz, E.J. *Immune evasion by human cytomegalovirus: lessons in immunology and cell biology.* Semin. Immunol. 13: 41-49, 2001.
22. Salvant, B.S., Fortunato, E.A., and Spector, D.H. *Cell cycle dysregulation by human cytomegalovirus: influence of the cell cycle phase at the time of infection and effects on cyclin transcription.* J. Virol., 72: 3729-3741, 1998.
23. Lokensgard, J.R., Cheeran, M.C., Gekker, G., Hu, S., Chao, C.C., and Perterson, P.K. *Human cytomegalovirus replication and modulation of apoptosis in astrocytes.* J. Hum. Virol., 2: 91-101, 1999.
24. Cinatl, J., Jr., Kotchetkov, R., Scholz, M., Cinatl, J., Vogel, J.U., Driever, P.H., and Doerr, H.W. *Human cytomegalovirus infection decreases expression of thrombospondin-1 independent of the tumor suppressor protein p53.* Am. J. Pathol. 155: 285-292, 1999.
25. Speir, E., Modali, R., Huang, E.S., Leon, M.B., Shawl, F., Finkel, T., and Epstein, S.E. *Potential role of human cytomegalovirus and p53 interaction in coronary restenosis.* Science (Wash. DC), 265: 391-394, 1994.
26. Scholz, M., Blaheta, R.A., et al. *Cytomegalovirus-infected neuroblastoma cells exhibit augmented invasiveness mediated by $\alpha_1\beta_5$ integrin (VLA-5).* Tissue Antigens, 55: 412-421, 2000.
27. Cobb, C.S., Harkins L., et al. *Human Cytomegalovirus Infection and Expression in Malignant Glioma.* Cancer Res., 62: 3347-3350, 2002.
28. Poland, S.D., Costello, P., et al. *Cytomegalovirus in the brain: in vitro infection of human brain-derived cells.* J. Infect. Dis., 162: 1252-1262, 1990.
29. Ogura, T., Tanaka, J., et al. *Human cytomegalovirus persistent infection in a human central nervous system cell line: production of a variant virus with different growth characteristics.* J. Gen. Virol., 67: 2605-2616, 1986.
30. Sinzger, C. and Jahn, G. *Human cytomegalovirus cell tropism and pathogenesis.* Intervirology, 39: 302-319, 1996.

31. Stenberg, R.M., Depto, A.S., et al. *Regulated expression of early and late RNAs and proteins from the human cytomegalovirus immediate-early gene region*. J. Virol., 63: 2699-2708, 1989.
32. Cherrington, J.M. and Mocarski, E.S. *Human cytomegalovirus ie1 transactivates the alpha promoter-enhancer via an 18-base-pair repeat element*. J. Virol., 63: 1435-1440, 1989.
33. Pizzorno, M.C., O'Hare, P., et al. *Trans-activation and autoregulation of gene expression by the immediate-early region 2 gene products of human cytomegalovirus*. J. Virol., 62: 1167-1179, 1988.
34. Hagemeyer, C., Walker, S.M., Sissons, P.J., and Sinclair, J.H. *The 72K IE1 and 80K IE2 proteins of human cytomegalovirus independently trans-activate the c-fos, c-myc, and hsp70 promoters via basal promoter elements*. J. Virol., 73: 2385-2393, 1992.
35. Hermiston, T.W., Malone, C.L., Witte, P.R., and Stinski, M.G. *Identification and characterization of the human cytomegalovirus immediate-early region 2 gene that stimulates gene expression from an inducible promoter*. J. Virol., 61: 3214-3221, 1987.
36. Hunninghake, G.W., Monick, M.M., Liu, B., and Stinski, M.F. *The promoter-regulatory region of the major immediate-early gene of human cytomegalovirus responds to T-lymphocyte stimulation and contains functional cyclic AMP-response elements*. J. Virol., 63: 3026-3033, 1989.
37. Caswell, R., Bryant, L., and Sinclair, J. *Human cytomegalovirus immediate-early 2 (IE2) protein can transactivate the human hsp70 promoter by alleviation of Dr1-mediated repression*. J. Virol., 70: 4028-4037, 1996.
38. Hayhurst, G.P., Bryant, L.A., et al. *CCAAT box-dependent activation of the TATA-less human DNA polymerase alpha promoter by the human cytomegalovirus 72-kilodalton major immediate-early protein*. J. Virol., 69: 182-188, 1995.
39. Schwartz, R., Sommer, J.H., Scully, A., and Spector, D.H. *Site-specific binding of the human cytomegalovirus IE2 86-kilodalton protein to an early gene promoter*. J. Virol., 68: 5613-5622, 1994.
40. Wade, M., Kowalik, T.F., et al. *E2F mediates dihydrofolate reductase promoter activation and multiprotein complex formation in human cytomegalovirus infection*. Mol. Cell. Biol., 12: 4364-4374, 1992.
41. Walker, S., Hagemeyer, C., Sissons, J.G., and Sinclair, J.H. *A 10-base-pair element of the human immunodeficiency virus type 1 long terminal repeat (LTR) is an absolute requirement for transactivation by the human cytomegalovirus 72-kilodalton IE1 protein but can be compensated for by other LTR regions in transactivation by the 80-kilodalton IE2 protein*. J. Virol., 66: 1543-1550, 1992.
42. Song, Y.J. and Stinski, M.F. *Inhibition of cell division by the human cytomegalovirus IE86 protein: Role of the p53 pathway or cyclin-dependent kinase 1/cyclin B1*. J. Virol., 79: 2597-2603, 2005.

43. Nevels, M., Paulua, C, and Shenk, T. *Human cytomegalovirus immediate-early 1 protein facilitates viral replication by antagonizing histone deacetylation*. PNAS, 101: 17234-17239, 2004.
44. Anders, D.G and McCue, L.A. *the human cytomegalovirus genes and proteins required for DNA synthesis*. Intervirology, 39: 378-388, 1996.
45. Gibson, W. *Structure and assembly of the virion*. Intervirology, 39: 389-400, 1996.
46. Spector, D.H. *Activation and regulation of human cytomegalovirus early genes*. Intervirology, 39: 361-377,1996.
47. Murphy, J.C., Fischle, W., Verdin, E., and Sinclair, J.H. *Control of cytomegalovirus lytic gene expression by histone acetylation*. EMBO, 21: 1112-1120,2002.
48. Castillo, J.P, and Kowalik, T.F. *Human cytomegalovirus immediate early proteins and cell growth control*. Gene, 290: 19-34, 2002.
49. Littler, E., Stuart A.D. *Human CMV UL97 open reading frame encodes a protein that phosphorylates the antiviral nucleoside analogue ganciclovir*. Nature, 358: 160-162, 1992.
50. Sullivan, V. Talarico, C.L. *A protein kinase homologue controls phosphorylation of ganciclovir in human CMV infected cells*. Nature, 358: 162-164, 1992.
51. Chee, M.S., Lawrence, G.L. *Alpha, beta, and gammaherpesvirus encode a putative phosphotransferase*. J. Gen. Virol., 70: 1151-1160, 1989.
52. He, Z., He, Y., et al . *The human CMV UL97 protein is a protein kinase that autophosphorylates on serines and threonines*. J .Virol., 71: 405-11, 1997.
53. Michel, D., Pavic, I., et al. *The UL97 gene product of human CMV is an early-late protein with nuclear localization but it is not a nucleoside kinase*. J. Virol., 70: 6340-6346, 1996
54. Pichard, M.N., Gao, N, et al. *A recombinant human CMV with large deletion of UL97 has severe replication deficiency*. J. Virol., 73: 5663-5670, 1999.
55. Marshall, M., Stein-Gerlach, M., et al. *Inhibitors of human CMV replication drastically reduce the activity of the viral protein kinase pUL97*. J. Gen. Virol., 82: 1439-1450, 2001.
56. Kouzarides, T. *Histone deacetylases and deacetylases in cell proliferation*. Curr. Opin. Genet. Dev., 9: 1999: 40-48.
57. Gray, SG, et al. *The human histone deacetylase family*. Exp. Cell Res., 262: 75-83, 2001
58. Jenuwein, I., and Allis, C.D. *Transplanting the histone code*. Science, 293: 1074-1080, 2001.
59. Wade, P.A. *Transcriptional control at regulatory checkpoints by histone deacetylases: molecular connections between cancer and chromatin*. Human Molecular Genetics,10: 693-698, 2001.
60. Cress, W.D. and Seto, E. *Histone deacetylases, transcriptional control and cancer*. J. Cell Physiology, 184: 1-16, 2000.

61. Chen, Ching-Shih. *Potent Phenylbutyrate Based Histone Deacetylase Inhibitors as Antitumor Agents*. RAID Application 2005.
62. Ueda H., Nakajima, H., Hori Y., et al. FR901228. *A Novel Antitumor Bicyclic Depsipeptide Produced by Chromobacterium Violaceum No 968: III Antitumor Activities on Experimental Tumors in Mice*. J. Antibiotics:315-323,1994.
63. Ueda, H., Nakajima, H.,Hori, Y. et al. *Action of FR901228, a Novel Antitumor Bicyclic Depsipeptide Produced by Chromobacterium Violaceum No. 968 on Ha-ras Transformed NIH3T3*. Biosci. Biotech.Biochem.:1579-1583,1994
64. Decision Network Notes. 94. Ref Type: Unpublished Work
65. Cinatl J Jr, Vogel JU, Cinatl J, Weber B, Rabenau H, Novak M, Kornhuber B, Doerr HW. *Long-term productive human cytomegalovirus infection of a human neuroblastoma cell line*. Int J Cancer. 1996 Jan 3;65(1):90-6.
66. Roychowdhury S, Peng R, Baiocchi RA, Bhatt D, Vourganti S, Grecula J, Gupta N, Eisenbeis CF, Nuovo GJ, Yang W, Schmalbrock P, Ferketich A, Moeschberger M, Porcu P, Barth RF, Caligiuri MA. *Experimental treatment of Epstein-Barr virus-associated primary central nervous system lymphoma*. Cancer Res. 63:965-71, 2003.

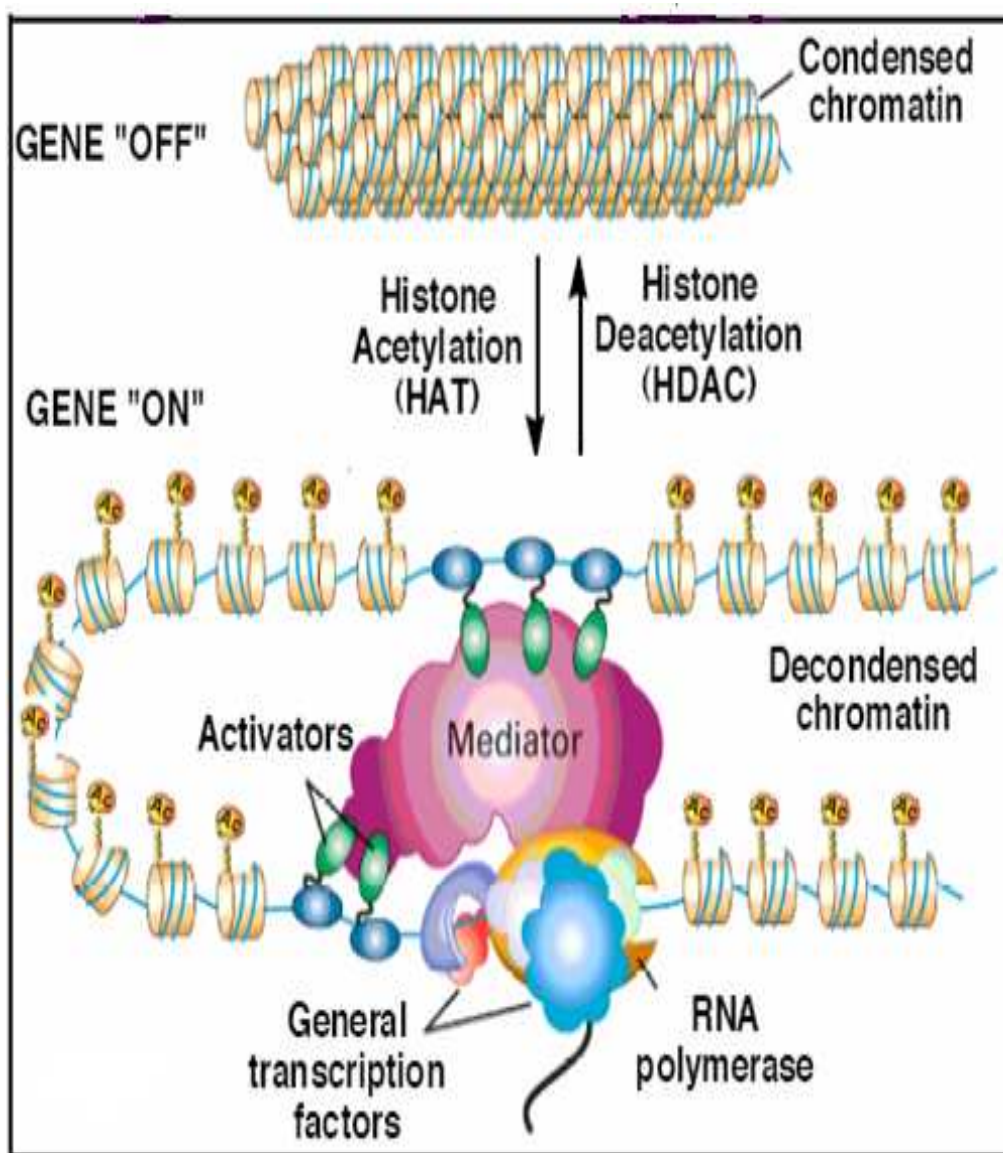


Figure 1: HAT v. HDAC activity. In the cell, histone acetyltransferases (HATs) promote relaxation of nucleosomal structures, allowing transcription to occur, while histone deacetylases (HDACs) promote chromatin compaction for transcriptional repression

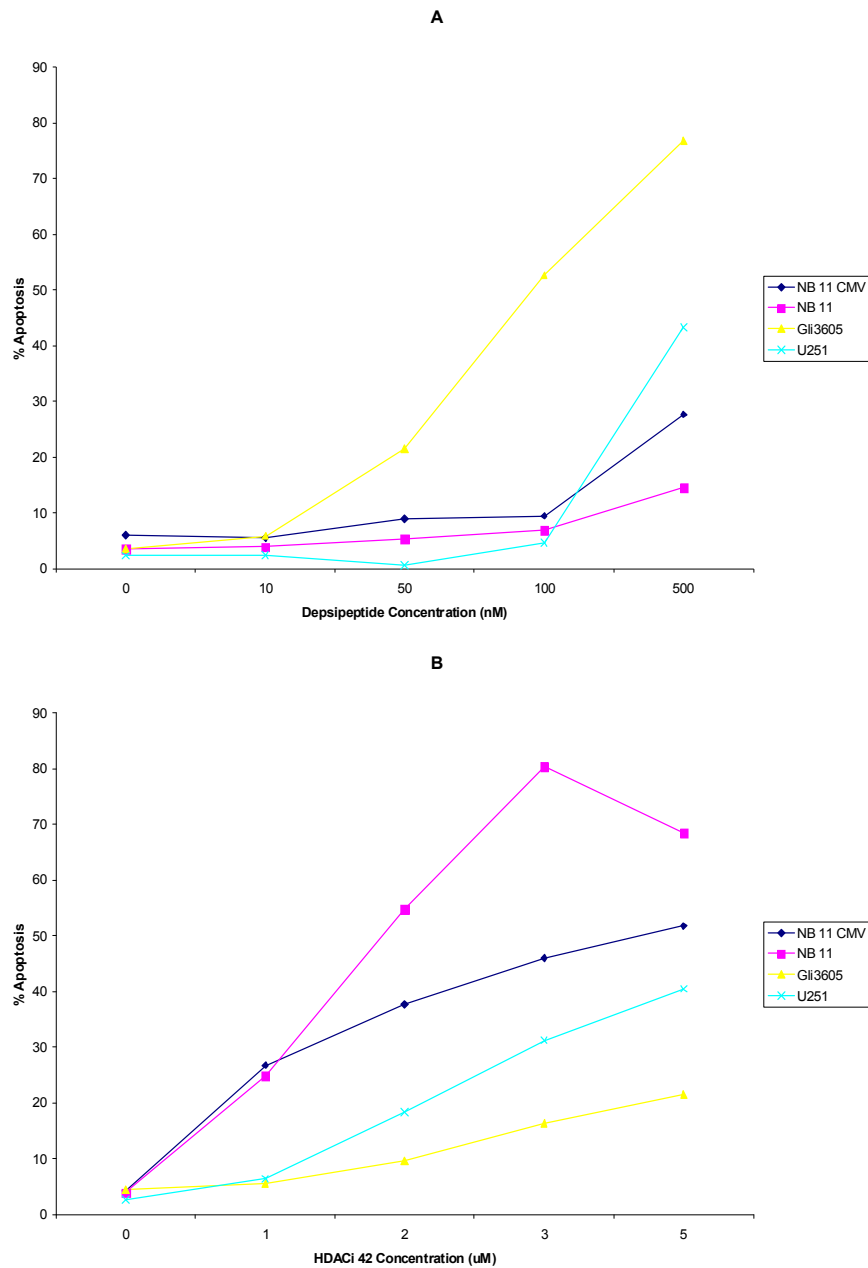


Figure 2: Dose-dependent HDACi induction of cell death at 48 hours. In (A), 0, 10, 50, 100, and 500 nM concentrations of depsipeptide were added and washed out after four hours. In (B), 0, 1, 2, 3, and 5 uM levels of HDACi 42 were added and left in. Both HDACi induced apoptosis.

HDACi 48hrs

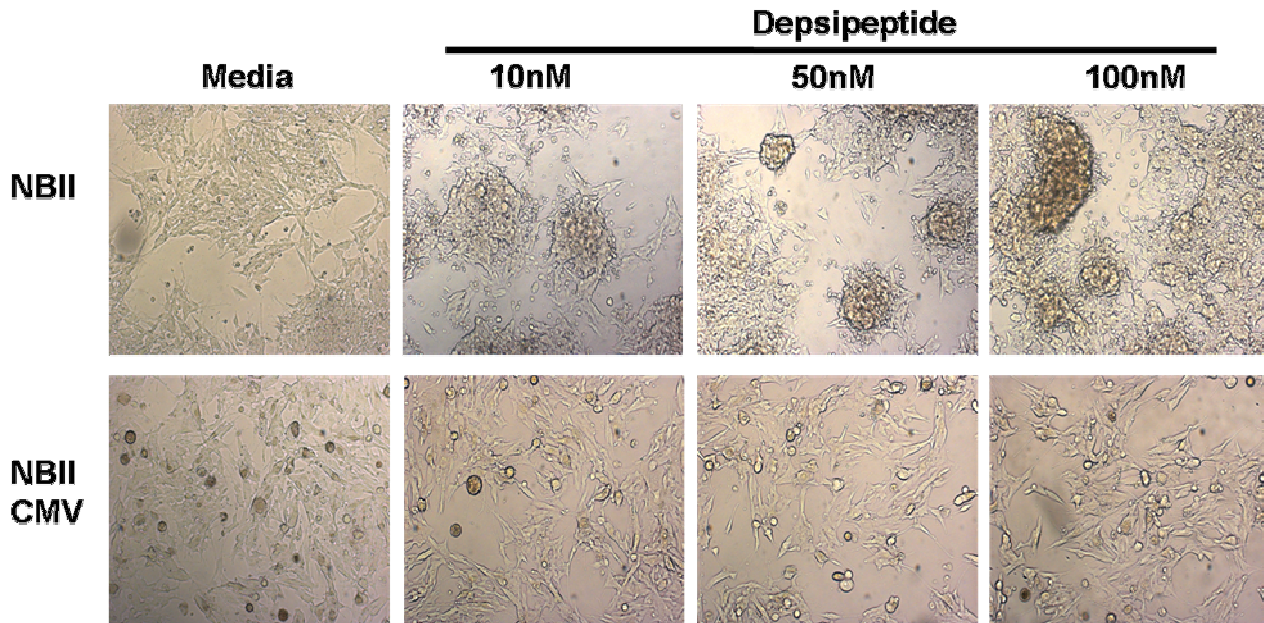


Figure 3: Morphology of depsipeptide treatment in NB11 and NB11 CMV. Adhered cells were incubated in drug for 4 hours, washed with PBS, and fresh growth media was added. Cells were viewed at 24 and 48 hours for morphological change. NB11 CMV cells appeared largely unaffected at 48hr compared to the parent line NB11 which demonstrated loss of adherence, cellular clumping and increased granularity.

HDACi 48hrs

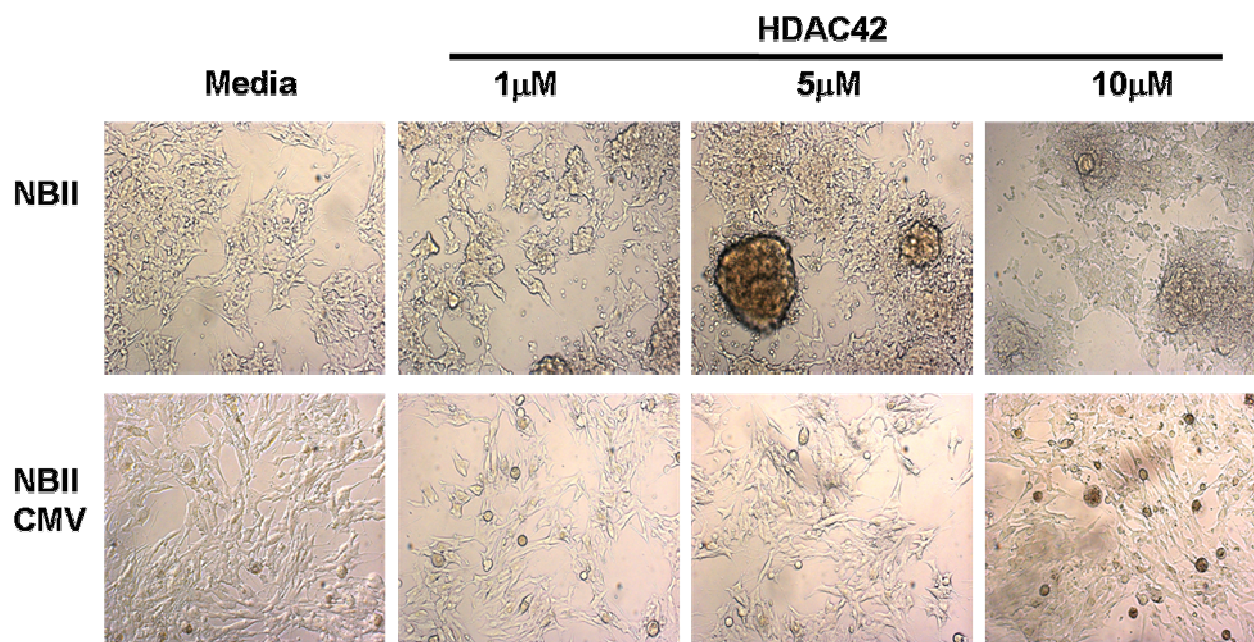
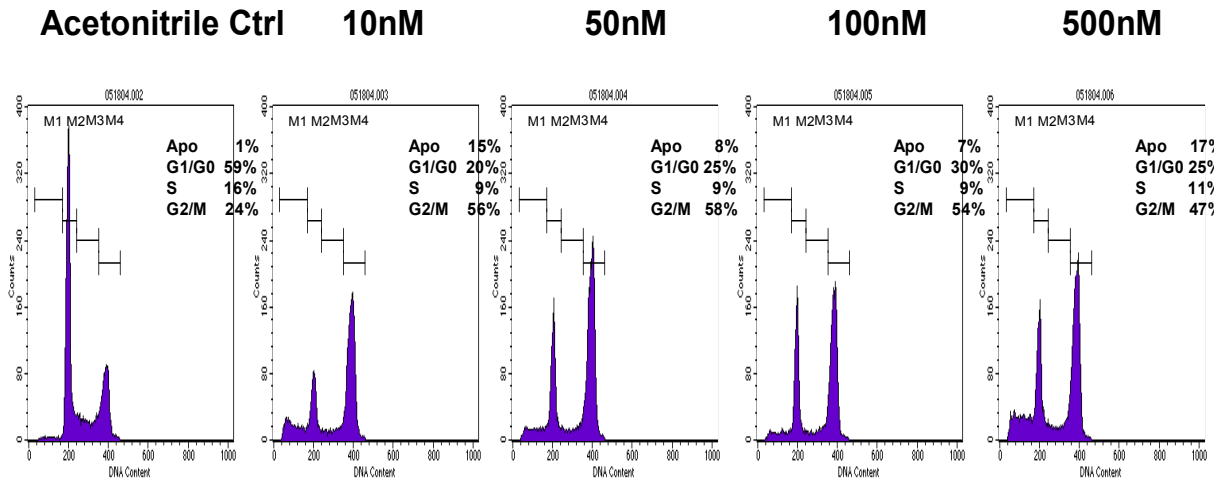


Figure 4: Morphology of HDACi 42 treatment in NB11 and NB11 CMV. Adhered cells were incubated in drug continuously. Cells were viewed at 24 and 48 hours for morphological change. Similar to results obtained with depsipeptide, NB11 CMV cells appeared largely unaffected at 48hr compared to the parent line NB11, which demonstrated loss of adherence, cellular clumping and increased granularity.

24hr

Depsipeptide



48hr

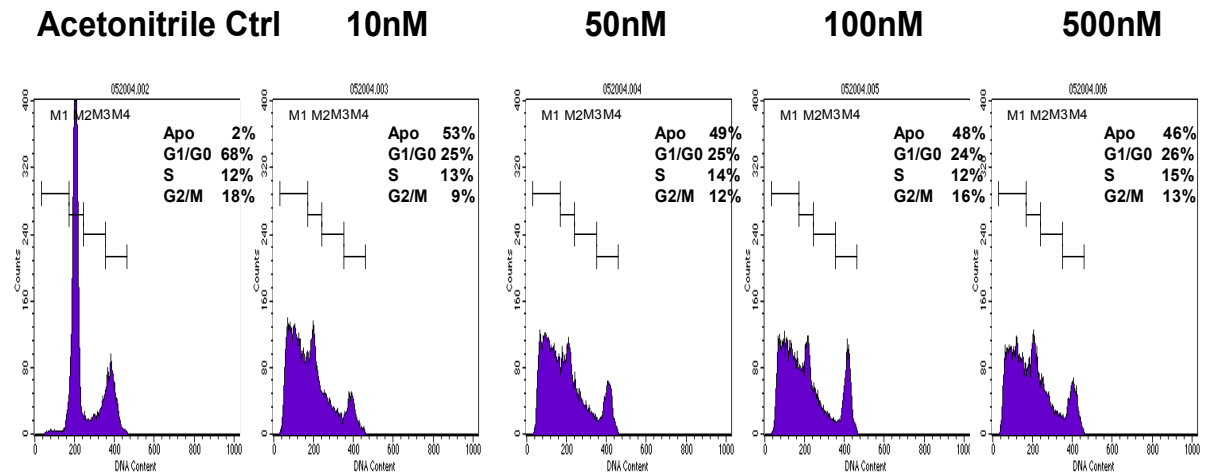


Figure 5: Depsipeptide induction of cell arrest and apoptosis in Gli3605. At 24 hours, induction of cell cycle arrest was seen in G2/M at all doses. By 48 hours, an average of 49% of the cells had become apoptotic for each concentration of 10, 50, 100, and 500 nM.

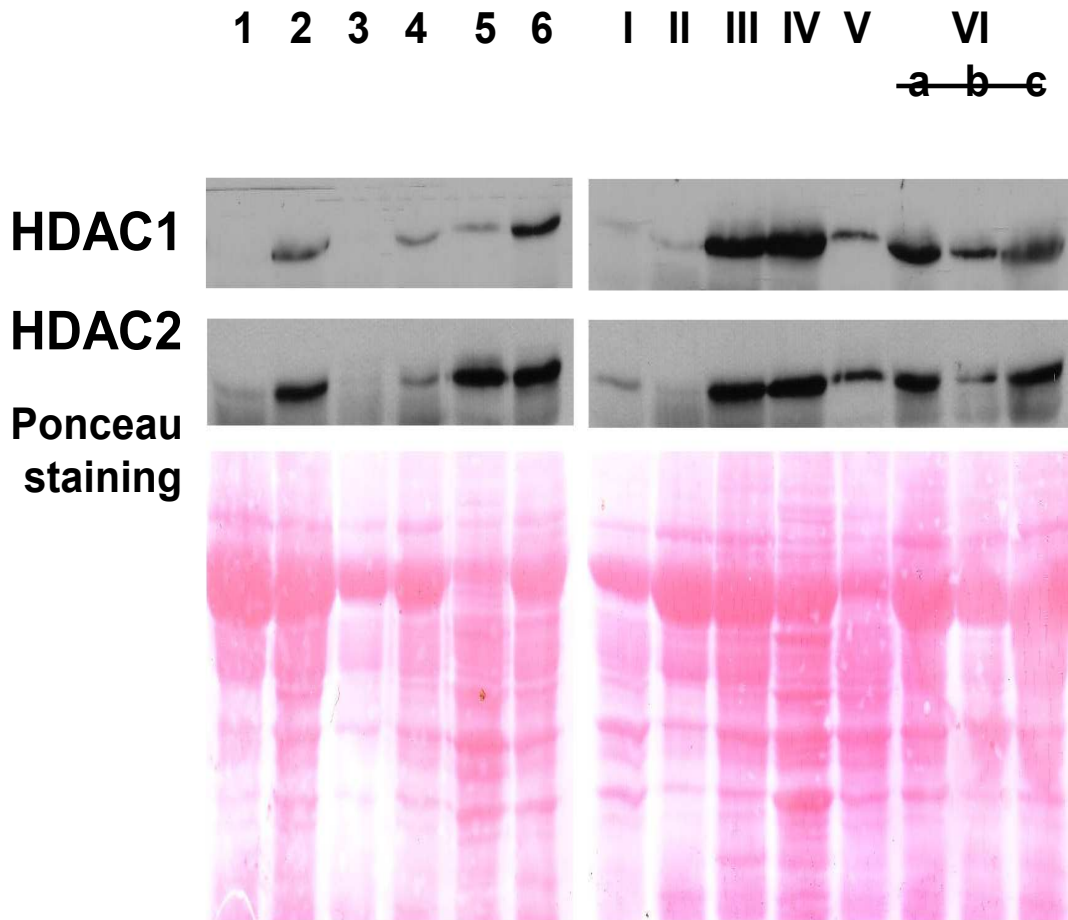


Figure 6: HDAC1 and HDAC2 protein expression in human brain tumors. Both proteins were increasingly expressed in tumor cells, as shown by Western Blot and Ponceau staining. Samples obtained from twelve patients, with three from patient VI analyzed (courtesy of Dr. Ennio Chiocca, Department of Neurological Surgery, OSU College of Medicine and Public Health).

Morphology

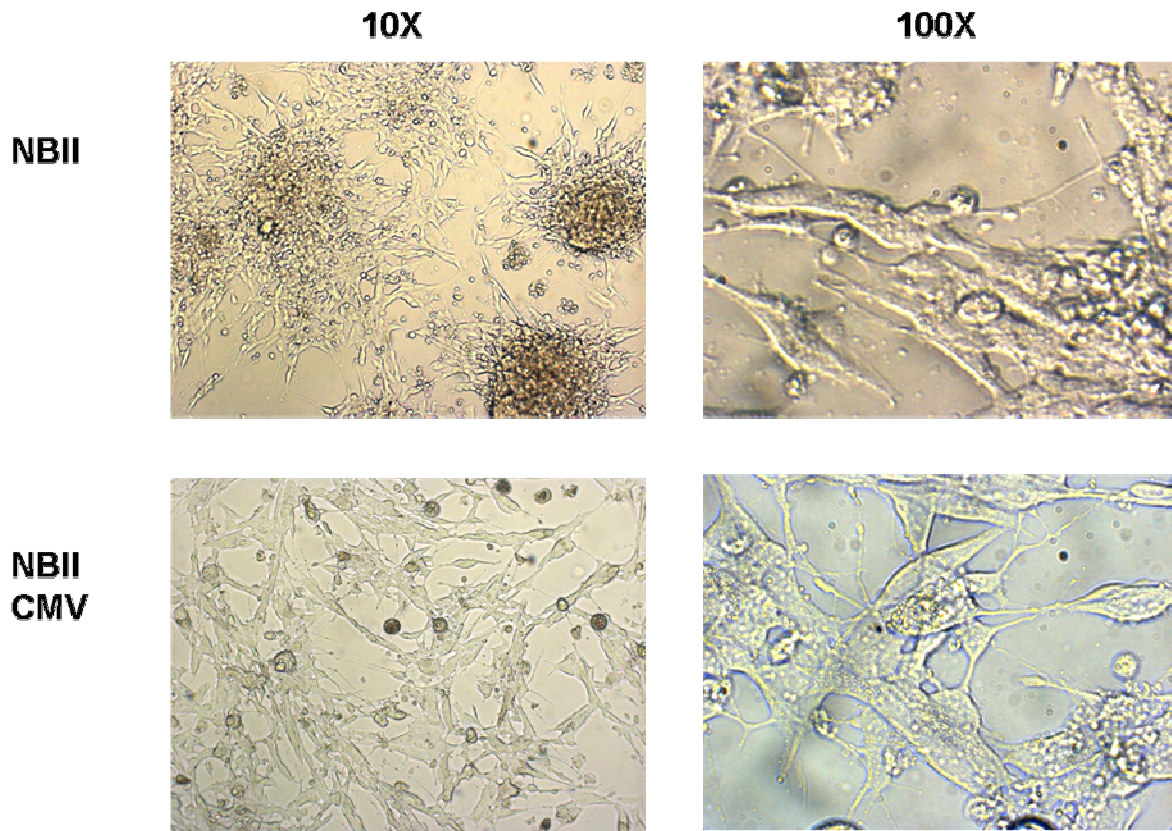
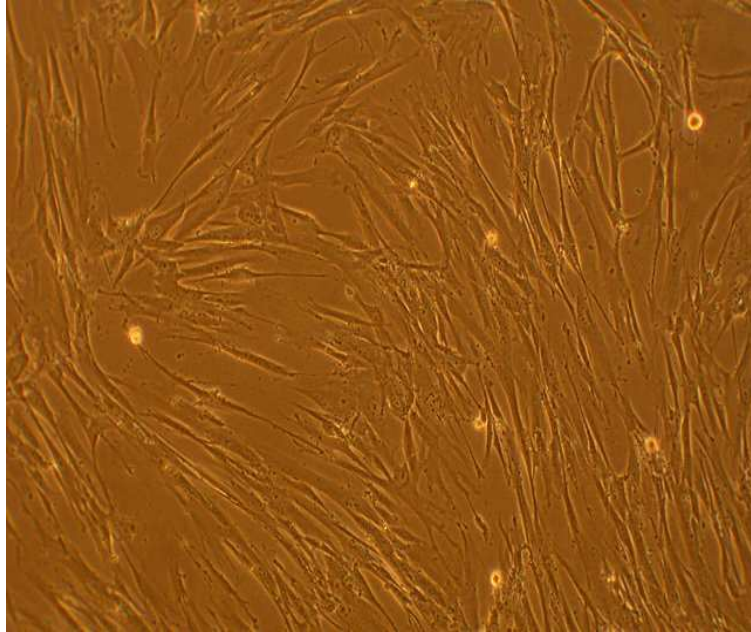


Figure 7: Morphology of NB11 and NB11 CMV cells. The NB11 line demonstrates loss of contact inhibition, growing in foci, and spindle-like morphology, while the CMV+ converted NB11 line shows larger size, lack of foci, enhanced syncytia formation.

A



B

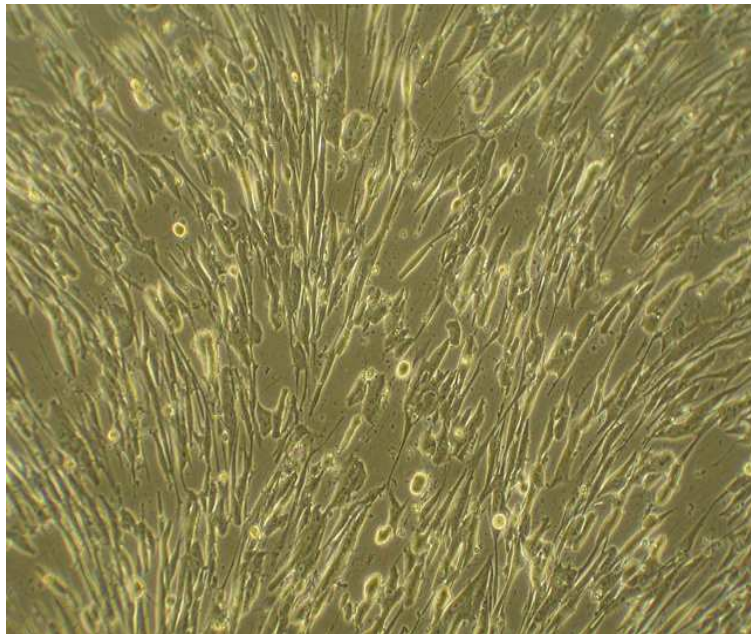


Figure 8: CMV alteration of fibroblast morphology.

Normal fibroblasts retain a long, flat, spindle-like shape (A). CMV causes fibroblasts to draw in their cellular extensions and develop a more rounded, raised morphology (B).

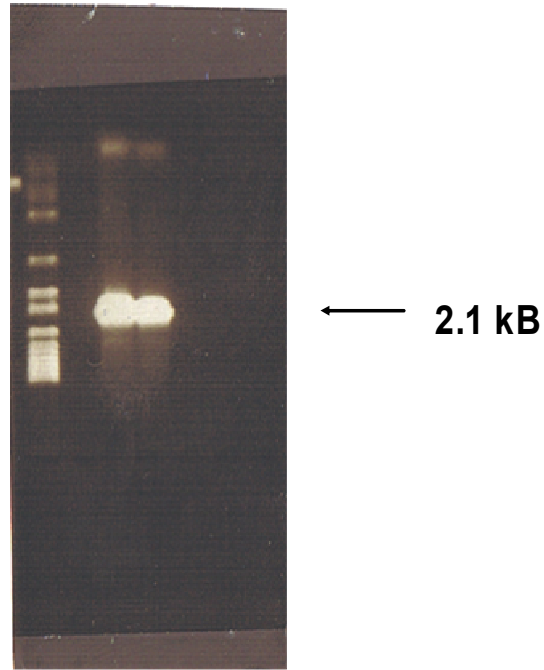


Figure 9: PCR replication of the UL97 gene product. CMV cDNA was isolated from AD169 infected fibroblasts, and UL97 was amplified. The 2.1 kB products are visible in lanes 2 and 3 of the 1% agarose gel.

Marker

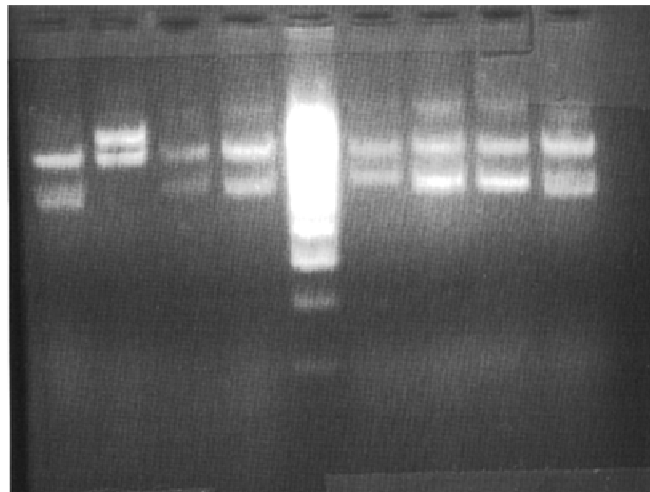


Figure 10: Determination of vectors containing insert. Samples of colonies growing in TB+Amp tubes were lysed with phenochloroform. The resulting aqueous layer was loaded on a 1% agarose gel with Supercoil DNA marker. All colonies were selected for mini preps.

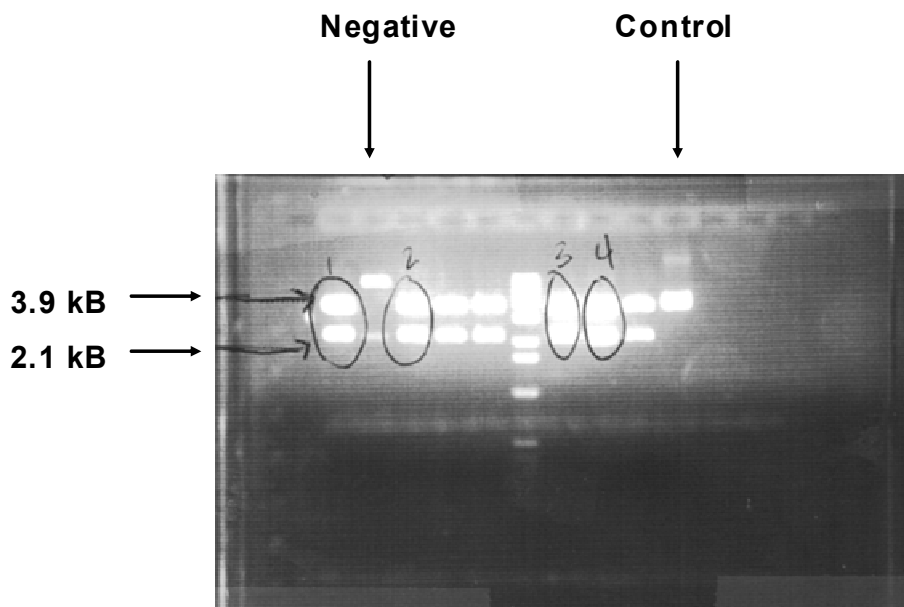


Figure 11: Mini prep for determination of correct insert size. Eight samples were mini prepped and subsequently digested with EcoRI to verify 2.1 kB size of the UL97 insert and 3.9 kB TOPO^R vector size. Seven colonies were confirmed, and four were selected for sequencing.

ECOR1 (gaattc)

U1-T3

ACT GCAGCTACGATT CGCOCT TCCG**GATTCATGTCCTCCGCAC**TTCCGGT CT CGGGCT CGCT CGGC
CT CGCT CGGAACGACGACT GAGGGCT GGGATCCGCCGCCAT T GCCT CGT CCCAGCAGGGCGCGCC
GGCGCCA GT GGAT GCGCGAAGCT GCGCAGGCCGCCGCT CAAGCCGCGGT GCAAGCCGCGCA GGC
CGCCGCCGCTCAGGT CGCCCA GGCT CACGT CGAT GAA GACGAGGT CGT GGATCT GAT GGCCGACGA
GGCCGGCGGGCGGCGT CACCACTTT GACCA COCT GAGTT CCGT CAGCA CAACCAOCT GCTT GGACA
CGCGACTT TTT CC GCAT GCGTT CGAAAT GACGT GAT GCCT GACGGA GAAAAAGAGCAGCGGCTT CG
GACAA GGA GAACCT GCGT CGGCCCGT GGT GCCGT CCACGTCGT CTCGCGGCA GCGCCGCCA GCGG
CGACGGTT ACCACGGCTT GCGCT GCGCGAA AOCCTCGGCCAT GT GGTCGTT CAGT ACGAT CGCGA
CGCGACGT GACCA GCGTACGCCGCGCCT CTT CACGGCGGCA GCGA CCCCT CGGACA GCGT GA
GCGGGCT CCGCGGT GACGCAAA GCGCCGTT GCCT CCGCGTT GGT GT CGCT GGCCCGCA CCCCGC
T GGT GCGACGT CT GT GCGGGCT GACGCGGT GCT CGAA GAAAA CGACGT GGAGCT GGCCCGCG
AAGT CAGGACA GCGCCT GGCAT CGGCCCGGCCGCGTT CCGCAGCCGCT CGGCGGT AGTT CCGGGA
AGAATCCGCCACGGCGGGGA GGGCGA TCCCA GTT CACGA GCACA TTT GCATT GGA CCT GGTT OCAC
GGACGGTT CACCCAGTT CCATCCGGGCTAACGGCA CCCCGGGT AGTTTTT GGCCTT ACGAT CCGG
GCT GGGAGCT CTAATT CT CAACGT CT GT CCACGT GCCAAGAGAGAAATTTT GGCAAAA GAACCT GTA
T GCCT GGACT GGAAC

U1-T7 (Xho 1 ctgag)

AGTAATAGGCGGCGGTATT CGCCCTT GGC**CTCGAGTTACT**CGGGGACA GTT GGCGGCA GT CACCG
T CAAGGT CCT CCT CGCAGATTAT GCT GGT GGT GCGCCGAAA GCGGTTAT ATAAT ACAGCCCGT CGC
T CGT GGCCAA CAGACGCT OCACGTT CTTT CT GCGCT ATT CGT GCAGCAT GGT CT GCGAGCAT TCCT G
GT AGAA GCGGGCAAAA GCGCGTACGCGACAC GAGGACAT CTT GGCCT CCACAAA GCGCAGCGT GT G
CGACACCA GCGCGGCGCCAT GCT CGCCCA GGA GACAGCGCCGT AGCTCATTT GCGCCGCA GAC
T GAGCAGACA GCGGT CGGAGCA GT GCGT GA GCTT GCGGTT CT CCAACGCGCGGCA GCGCCGCGCG
GCGT GCTT AAA GAGCAACGCCT CCGT GCOCAT GCGCA CCT CGT CCA GACCGCGCGGCT CCAACAGC
CCGAT GAGGCAAAA GCCAGCACGTT CCCCAGCGCCGACA GCT CCGACAT GCAATAACGCCGTAGA
CCGGCTACGGGGA AACGCGCGT GCGGGT CGCAGAT GAGCA GCTT CT CAGCGGCAT GGT CCGGAA
AGCAGGGT GGTAACATT CGCGCAGACGGT GCGAGCAT TGGGGAT GCGGCGCGCCGT GCCCGT CT
CCT GAAA GACGGCCACA CAGCGCTCGTT GTAAT CCGGATAGGGCT CGCT GAGGCT GT AAT CGCACA
GCGCGGCGCGCAGAT CT CGCT GGGGTT GT GCGGGTT CACGT CGAT GAGCACGTT CAT GGGT GTAA
T GT CAAA GT GGCAT ACACGACACT GGT GATT GAGAAT TT GAT AGCGT CGGCCACGT GCAAAGGCACG
TCGGT AGCT GT CGAT GACGCCAGCTT CCACT GGT CGT GAT GAACAT GT CTT GTT GGAACCTT CGAT
GT ACTT GT GACGTTT GCAACAACAGCACCCGT GGCCGT GAGCAAA CCGCGGT GACGCCCGTACTA
CAAGCGACGGG

Figure 12: Sequencing of vector inserts. Clones with inserts of the correct size were sent for sequencing using M13 forward and reverse primers with T3 and T7 polymerases, and all clones returned 97-98% homology to the UL97 CMV protein kinase, as determined using NCBI Nucleotide Blast software.

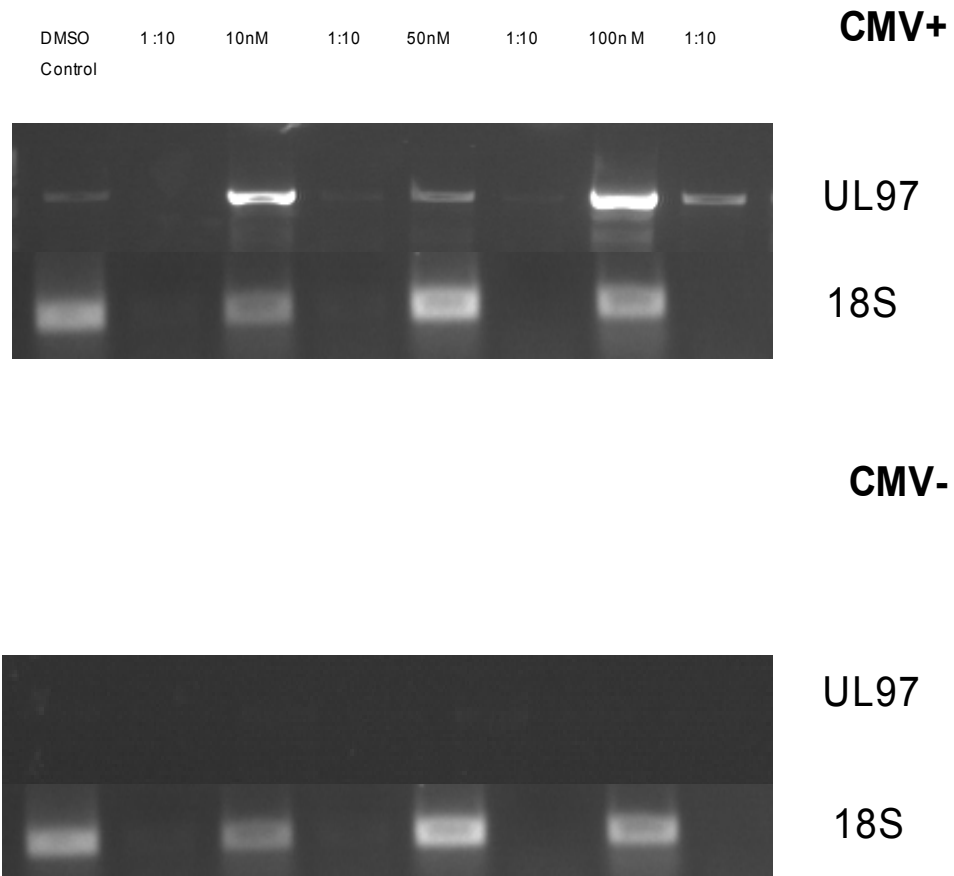


Figure 13: Depsipeptide induction of UL97 and 18S in NB11-CMV. At concentrations of 10, 50, and 100 nM, DP induced expression of the UL97 CMV and the cellular 18S proteins at 48 hours. In the CMV- line, NB11, no expression of UL97 was induced. Undiluted and 1:10 dilutions of cDNA were used for each PCR reaction, and samples were loaded on a 1% agarose gel.

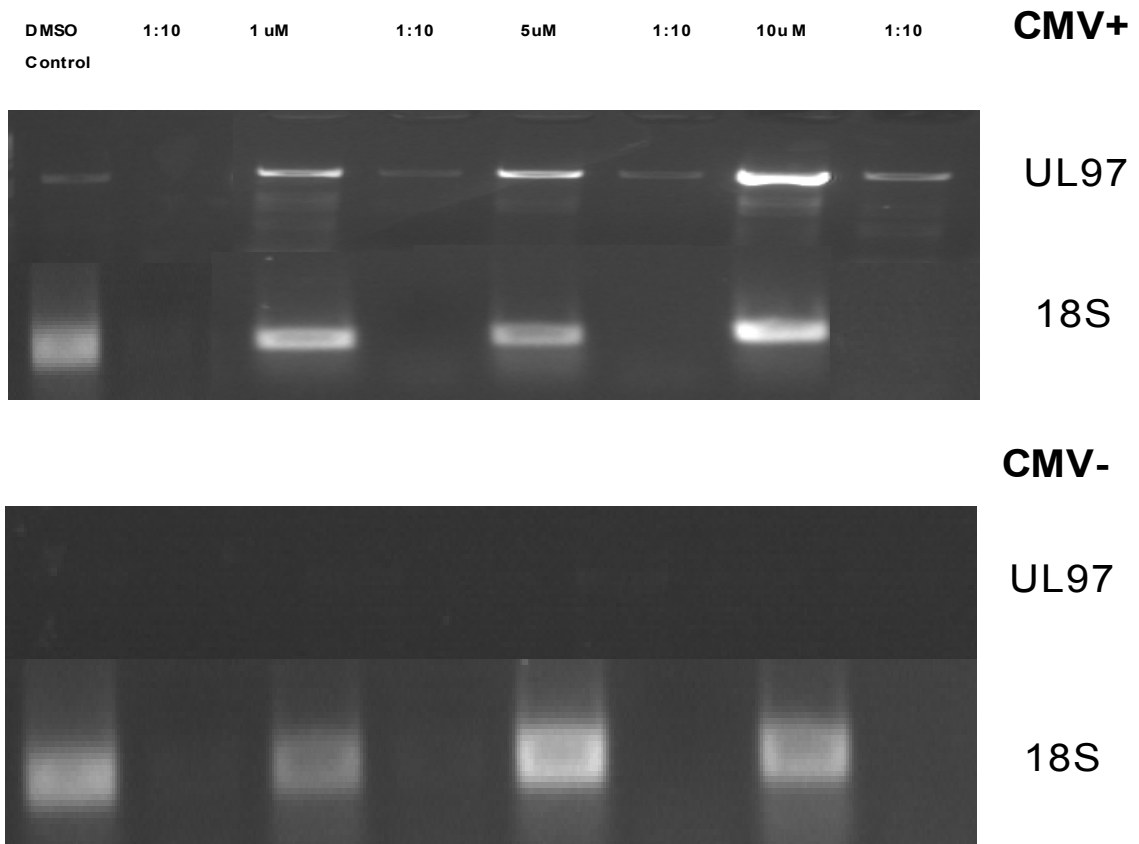


Figure 14: HDACi 42 induction of UL97 and 18S in NB11 CMV. At concentrations of 1, 5, and 10 uM, HDACi 42 induced expression of the UL97 CMV and the cellular 18S proteins at 48 hours. In the CMV- line, NB11, no expression of UL97 was induced. Undiluted and 1:10 dilutions of cDNA were used for each PCR reaction, and products were loaded on a 1% agarose gel.

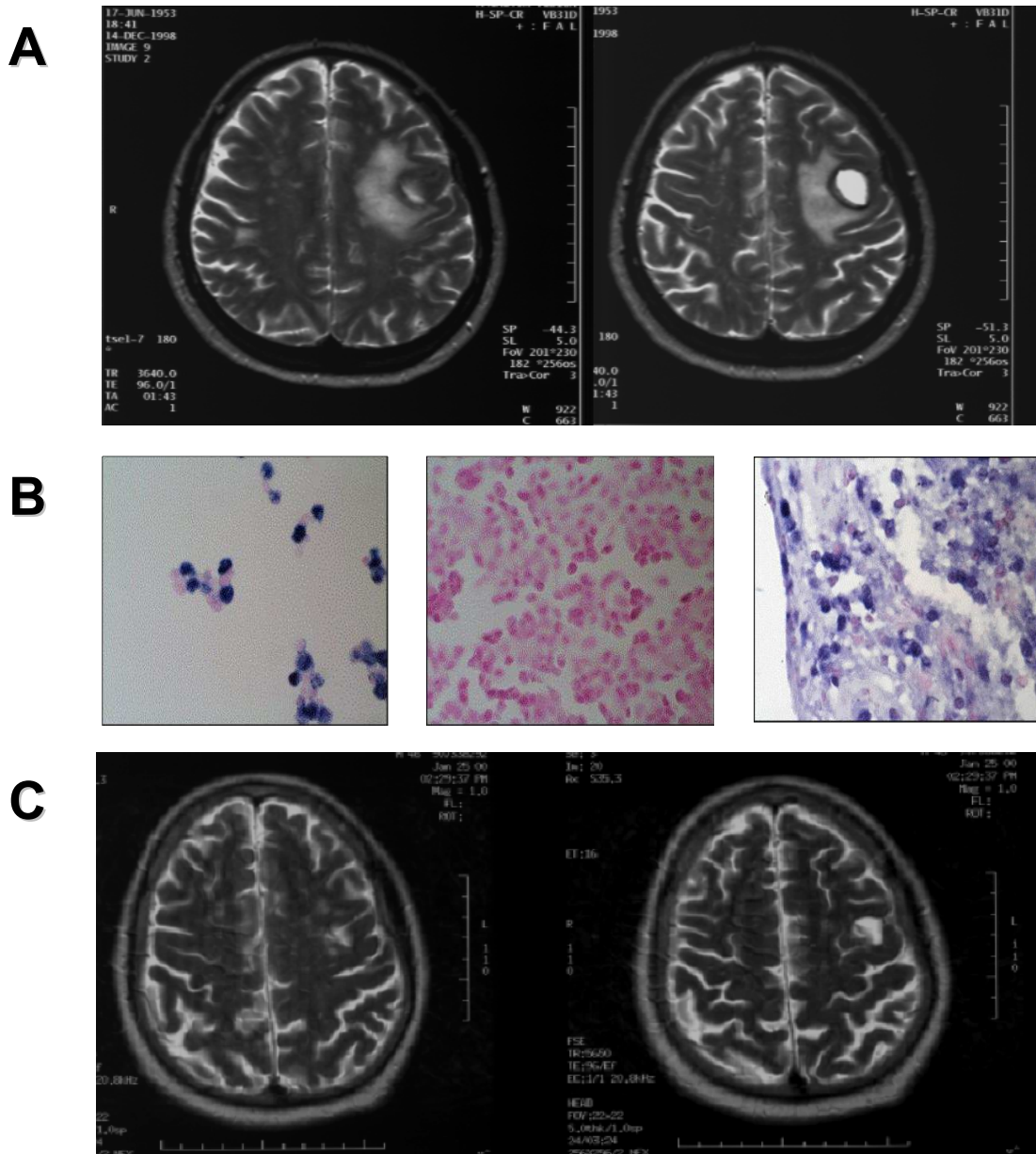


Figure 15: PCNSL and consequences of EBV thymidine kinase expression. Primary CNS lymphoma in a patient with EBV+ lymphoproliferative disease. (A) Multiple tumor foci throughout the brain parenchyma were found on diagnosis. (B) Stereotactic core biopsy was performed showing EBV antigens and in-situ RT-PCR demonstrated the presence of the EBV ORF BXLF1, a viral thymidine kinase capable of phosphorylating the nucleoside analogue AZT. Left panel is a positive control (B95.8 cells), mid panel is negative control (EBV- osteosarcoma cell line), and right panel is the biopsy demonstrating multiple positive signals indicating abundant expression of the vTK gene product. (C) Following 2 wks of high dose AZT/GCV, this patient attained a complete response and is now cured of his disease.

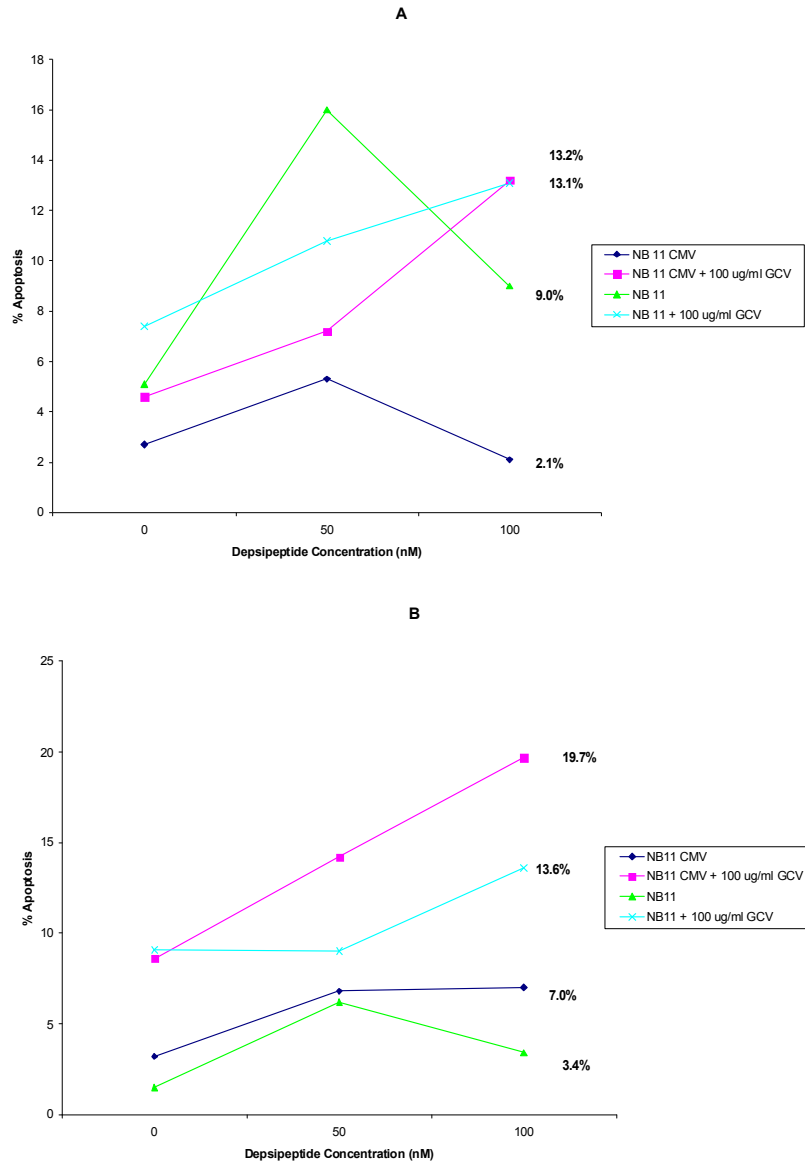


Figure 16: Ganciclovir addition increases apoptosis. Addition of 100 ug/ml GCV resulted in increased apoptosis at 48 hours (A) and 72 hours (B) compared to depsipeptide alone. Between NB11 and NB11 CMV, there was greater effect in the CMV+ line.

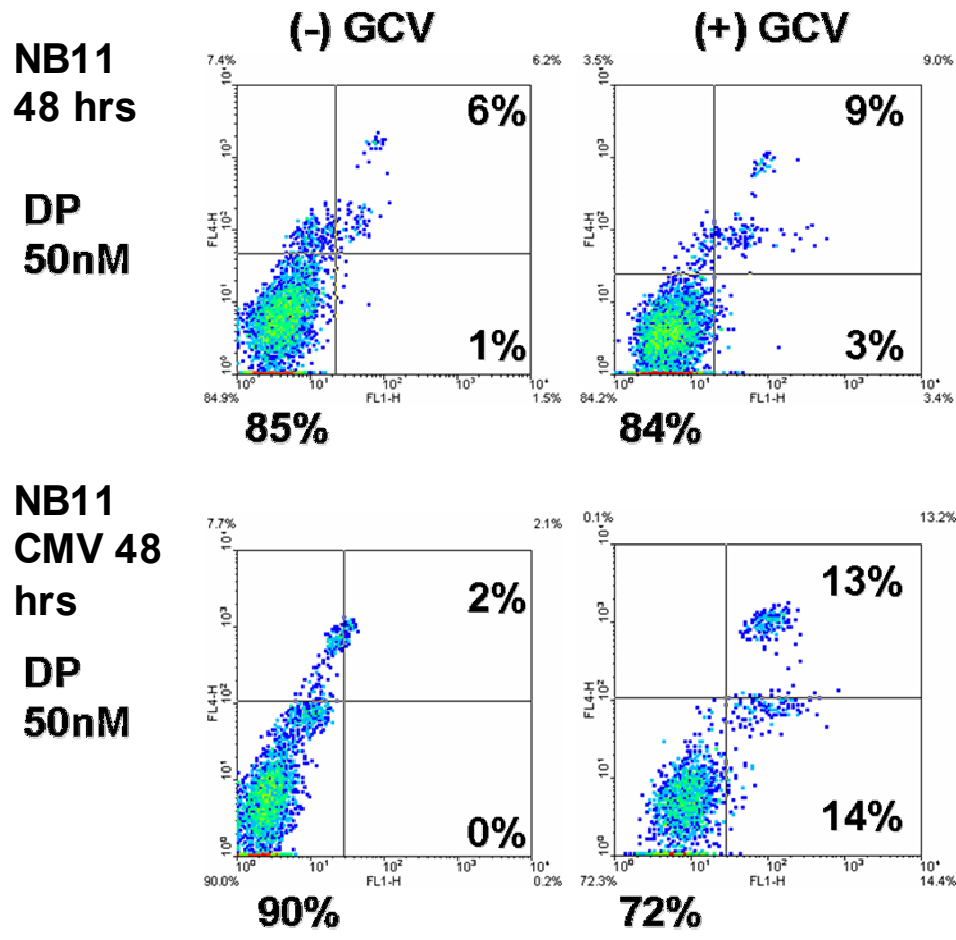


Figure 17: Ganciclovir addition increases apoptosis (expt 2). NBII CMV+ cells demonstrate enhanced apoptosis by Ann/ToprollI FACS assay. Cells were treated with DP (50nM) for 4 hours, washed, and subsequently placed in absence or presence of GCV (100ug/ml). CMV+ cells that demonstrated increased UL97 transcript following treatment with HDAC-I were more susceptible to GCV-induced cell death. Top panel NBII and bottom panel is NBII CMV

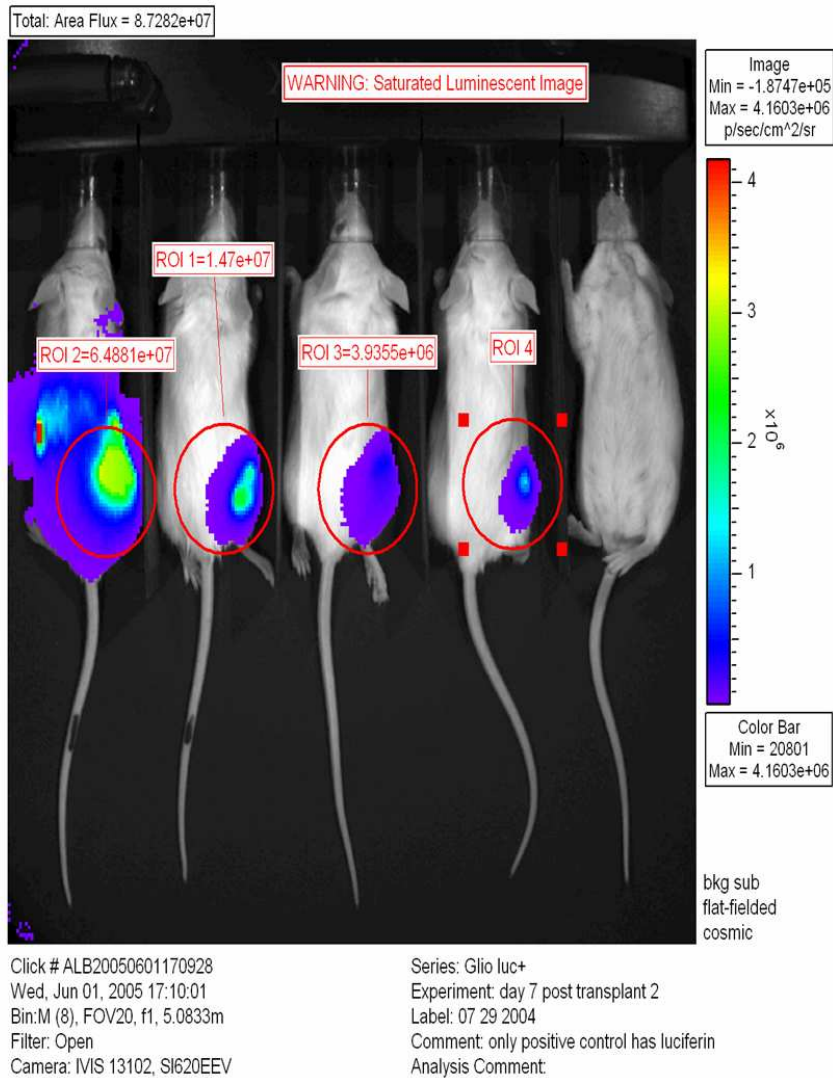


Figure 18: Gli3605 tumor cells expressing luciferin in animal model. Gli3605 cells constitutively expressing the luciferin gene were injected into the thigh of the animal model and allowed to proliferate. These tumors will be targeted with depsipeptide and HDACi 42.